

UNCLASSIFIED

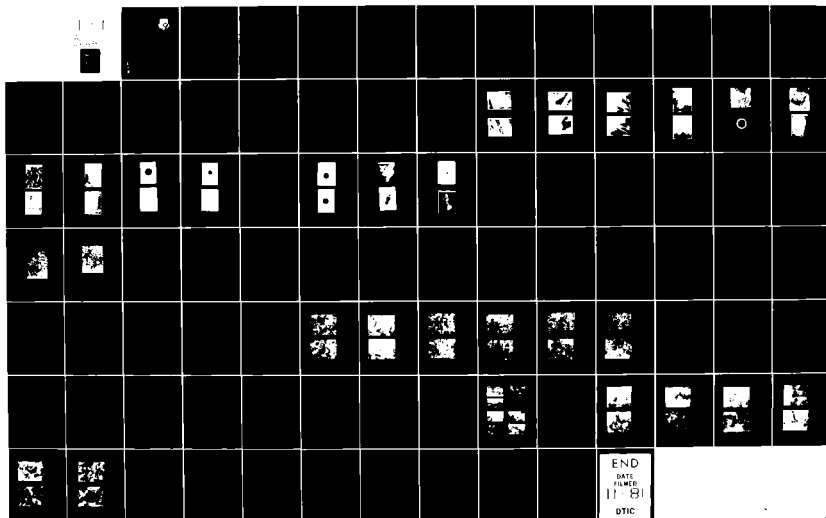
MAY 81 A G JACKSON, R E OMLOR, R J BACON

F33615-77-C-5008

SRL-6945

AFWAL-TR-81-4047

NL



AD A106351

(17)

APVAL-TR-81-4047

CHARACTERIZATION OF MICROSTRUCTURES



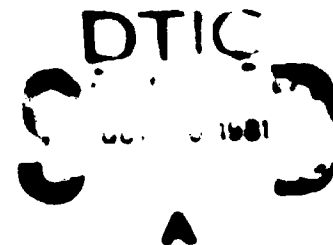
A. G. Jackson
K. E. Chior
K. J. Bacon
M. B. Strope

Research Applications Division
Systems Research Laboratories, Inc.
2800 Indian Ripple Road
Dayton, OH 45440

June 1981

Final Report for Period 1 May 1977 - 1 October 1980

Approved for public release; distribution unlimited



MATERIALS LABORATORY
AIR FORCE WRIGHT AERONAUTICAL LABORATORIES
AIR FORCE SYSTEMS DIVISION
WRIGHT-PATTERSON AIR FORCE BASE, OH 45433

AD A106351

81 10 87 274

NOTICE

When Government drawings, specifications, or other data are used for any purpose other than in connection with a definitely related Government procurement operation, the United States Government thereby incurs no responsibility nor any obligation whatsoever, and the fact that the government may have formulated, furnished, or in any way supplied the said drawings, specifications, or other data, is not to be regarded by implication or otherwise as in any manner licensing the holder or any other person or corporation, or conveying any rights or permission to manufacture, use, or sell any patented invention that may in any way be related thereto.

This report has been reviewed by the Office of Public Affairs (ASD/PA) and is releasable to the National Technical Information Service (NTIS). At NTIS, it will be available to the general public, including foreign nations.

This technical report has been reviewed and is approved for publication.



Charles Underwood
Project Monitor

FOR THE COMMANDER



William E. Thompson
Chief, Structural Metals Branch
Metals & Ceramics Division

If your address has changed, if you wish to be removed from our mailing list, or if the addressee is no longer employed by your organization please notify AFRL/MLL, WPAFB OH 45433 to help us maintain a current mailing list.

Copies of this report should not be returned unless return is required by security considerations, contractual obligations, or notice on a specific document.

FORM 100-100-100-100-100

UNCLASSIFIED

SECURITY CLASSIFICATION OF THIS PAGE (When Data Entered)

REPORT DOCUMENTATION PAGE		READ INSTRUCTIONS BEFORE COMPLETING FORM
1. AUTHOR (Last, First, Middle Initial)		2. TITLE (and Subtitle)
3. AUTHORING ORGANIZATION NAME(s)		4. PERFORMING ORGANIZATION NAME(s)
5. AUTHORING ORGANIZATION REPORT NUMBER		6. PERFORMING ORGANIZATION REPORT NUMBER
7. AUTHORING ORGANIZATION ADDRESS		8. PERFORMING ORGANIZATION ADDRESS
9. AUTHORING ORGANIZATION CITY, STATE, ZIP		10. PERFORMING ORGANIZATION CITY, STATE, ZIP
11. AUTHORING ORGANIZATION COUNTRY		12. PERFORMING ORGANIZATION COUNTRY
13. AUTHORING ORGANIZATION ABBREVIATION		14. PERFORMING ORGANIZATION ABBREVIATION
15. AUTHORING ORGANIZATION PHONE NUMBER		16. PERFORMING ORGANIZATION PHONE NUMBER
17. AUTHORING ORGANIZATION FAX NUMBER		18. PERFORMING ORGANIZATION FAX NUMBER
19. AUTHORING ORGANIZATION E-MAIL ADDRESS		20. PERFORMING ORGANIZATION E-MAIL ADDRESS
21. AUTHORING ORGANIZATION URL		22. PERFORMING ORGANIZATION URL
23. AUTHORING ORGANIZATION OTHER INFORMATION		24. PERFORMING ORGANIZATION OTHER INFORMATION
25. AUTHORING ORGANIZATION OTHER INFORMATION		26. PERFORMING ORGANIZATION OTHER INFORMATION
27. AUTHORING ORGANIZATION OTHER INFORMATION		28. PERFORMING ORGANIZATION OTHER INFORMATION
29. AUTHORING ORGANIZATION OTHER INFORMATION		30. PERFORMING ORGANIZATION OTHER INFORMATION
31. AUTHORING ORGANIZATION OTHER INFORMATION		32. PERFORMING ORGANIZATION OTHER INFORMATION
33. AUTHORING ORGANIZATION OTHER INFORMATION		34. PERFORMING ORGANIZATION OTHER INFORMATION
35. AUTHORING ORGANIZATION OTHER INFORMATION		36. PERFORMING ORGANIZATION OTHER INFORMATION
37. AUTHORING ORGANIZATION OTHER INFORMATION		38. PERFORMING ORGANIZATION OTHER INFORMATION
39. AUTHORING ORGANIZATION OTHER INFORMATION		40. PERFORMING ORGANIZATION OTHER INFORMATION
41. AUTHORING ORGANIZATION OTHER INFORMATION		42. PERFORMING ORGANIZATION OTHER INFORMATION
43. AUTHORING ORGANIZATION OTHER INFORMATION		44. PERFORMING ORGANIZATION OTHER INFORMATION
45. AUTHORING ORGANIZATION OTHER INFORMATION		46. PERFORMING ORGANIZATION OTHER INFORMATION
47. AUTHORING ORGANIZATION OTHER INFORMATION		48. PERFORMING ORGANIZATION OTHER INFORMATION
49. AUTHORING ORGANIZATION OTHER INFORMATION		50. PERFORMING ORGANIZATION OTHER INFORMATION
51. AUTHORING ORGANIZATION OTHER INFORMATION		52. PERFORMING ORGANIZATION OTHER INFORMATION
53. AUTHORING ORGANIZATION OTHER INFORMATION		54. PERFORMING ORGANIZATION OTHER INFORMATION
55. AUTHORING ORGANIZATION OTHER INFORMATION		56. PERFORMING ORGANIZATION OTHER INFORMATION
57. AUTHORING ORGANIZATION OTHER INFORMATION		58. PERFORMING ORGANIZATION OTHER INFORMATION
59. AUTHORING ORGANIZATION OTHER INFORMATION		60. PERFORMING ORGANIZATION OTHER INFORMATION
61. AUTHORING ORGANIZATION OTHER INFORMATION		62. PERFORMING ORGANIZATION OTHER INFORMATION
63. AUTHORING ORGANIZATION OTHER INFORMATION		64. PERFORMING ORGANIZATION OTHER INFORMATION
65. AUTHORING ORGANIZATION OTHER INFORMATION		66. PERFORMING ORGANIZATION OTHER INFORMATION
67. AUTHORING ORGANIZATION OTHER INFORMATION		68. PERFORMING ORGANIZATION OTHER INFORMATION
69. AUTHORING ORGANIZATION OTHER INFORMATION		70. PERFORMING ORGANIZATION OTHER INFORMATION
71. AUTHORING ORGANIZATION OTHER INFORMATION		72. PERFORMING ORGANIZATION OTHER INFORMATION
73. AUTHORING ORGANIZATION OTHER INFORMATION		74. PERFORMING ORGANIZATION OTHER INFORMATION
75. AUTHORING ORGANIZATION OTHER INFORMATION		76. PERFORMING ORGANIZATION OTHER INFORMATION
77. AUTHORING ORGANIZATION OTHER INFORMATION		78. PERFORMING ORGANIZATION OTHER INFORMATION
79. AUTHORING ORGANIZATION OTHER INFORMATION		80. PERFORMING ORGANIZATION OTHER INFORMATION
81. AUTHORING ORGANIZATION OTHER INFORMATION		82. PERFORMING ORGANIZATION OTHER INFORMATION
83. AUTHORING ORGANIZATION OTHER INFORMATION		84. PERFORMING ORGANIZATION OTHER INFORMATION
85. AUTHORING ORGANIZATION OTHER INFORMATION		86. PERFORMING ORGANIZATION OTHER INFORMATION
87. AUTHORING ORGANIZATION OTHER INFORMATION		88. PERFORMING ORGANIZATION OTHER INFORMATION
89. AUTHORING ORGANIZATION OTHER INFORMATION		90. PERFORMING ORGANIZATION OTHER INFORMATION
91. AUTHORING ORGANIZATION OTHER INFORMATION		92. PERFORMING ORGANIZATION OTHER INFORMATION
93. AUTHORING ORGANIZATION OTHER INFORMATION		94. PERFORMING ORGANIZATION OTHER INFORMATION
95. AUTHORING ORGANIZATION OTHER INFORMATION		96. PERFORMING ORGANIZATION OTHER INFORMATION
97. AUTHORING ORGANIZATION OTHER INFORMATION		98. PERFORMING ORGANIZATION OTHER INFORMATION
99. AUTHORING ORGANIZATION OTHER INFORMATION		100. PERFORMING ORGANIZATION OTHER INFORMATION

DO 1000 1473

UNCLASSIFIED

UNCLASSIFIED

SECURITY CLASSIFICATION OF THIS PAGE (When Data Entered)

UNCLASSIFIED

SECURITY CLASSIFICATION OF THIS PAGE(When Data Entered)

20. Abstract continued

PM alloy, formulation of a color micrograph method for titanium-hydride determination, and use of new microcomputer methods for stereological analyses of microstructures. The Materials Characterization Facility is described in terms of the physical plant and the methods of operation used in accomplishing the research on microstructures.

UNCLASSIFIED

SECURITY CLASSIFICATION OF THIS PAGE(When Data Entered)

PREFACE

This final report was prepared by the Research Applications Division of Systems Research Laboratories, Inc., 2800 Indian Ripple Road, Dayton, OH 45440, under Contract No. F33615-77-C-5008, Project 2418, Task 02, Work Unit 01, with Mr. Charles Underwood (AFWAL/MLIS) as Government Project Monitor. The research was conducted by Mr. Allen G. Jackson, Mr. Ralph E. Omlor, Mr. Richard J. Bacon, Mr. M. Brewster Strobe, Ms. Pamela F. Lloyd, Mr. Robert D. Brodecki, Mr. Walter J. Custer, Mr. Fritz O. Deutscher, Ms. J. Cheryl Conley, and Mr. James G. Paine. This report describes efforts performed during the period 1 May 1977 - 1 October 1980. The report was submitted in February 1981.

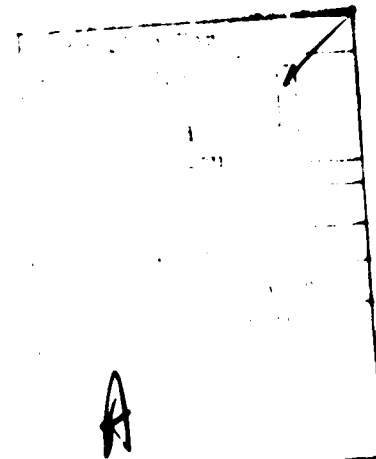


TABLE OF CONTENTS

<u>Section</u>	<u>Page</u>
1 INTRODUCTION	1
2 THE MATERIALS CHARACTERIZATION FACILITY (MCF)	5
PHYSICAL DESCRIPTION OF THE FACILITY	5
OPERATION AND MANAGEMENT OF FACILITY	6
3 RESEARCH ACCOMPLISHED	7
PRESENTATIONS AND PUBLICATIONS	7
HIGHLIGHTS OF SPECIFIC MCF ACTIVITIES	8
Electron-Optics	9
Transmission Electron Microscopy	9
Scanning Electron Microscopy	21
Electron-Probe Microanalysis	25
Metallography and Photo Labs	29
Quantitative Metallography	36
Special Projects	46
REFERENCES	82

LIST OF ILLUSTRATIONS

Figure		Page
1	Ti-6-4 Undeformed Dehydrogenated Specimen Showing Slip.	11
2	Ti-6-4 Undeformed Dehydrogenated Specimen Showing Dislocation Network.	11
3	Bright Field of Ti-6-4 95H Platelets.	12
4	Dark Field of Ti-6-4. Same area as Fig. 3.	12
5a	Initial Condition of Ti-6Al 4V + H Specimen.	13
5b	Effect of Heating at 200°C upon Dislocations Present in the Hydride.	13
6a	Initial Condition of Ti-6Al-4V + H Specimen.	14
6b	Effect of Heating at 350°C upon Dislocations Present in the Hydride.	14
7	SEM Photomicrograph Taken on the ETEC.	15
8	Lettered Grid Used to Locate Areas of a Specimen.	15
9	SEM Micrograph of a Pore and Its Cracks.	16
10	TEM Replica Showing a Pore and Its Cracks.	16
11	Large Carbide Particle.	17
12	Shear γ' Near the Pore.	17
13	Major Crack and Parallel Slip Lines.	18
14	Crack From Pore to Edge and Sheared γ' .	18
15	Blend of ABPBI/PBT Cast onto Grid.	19
16	Single Crystal of ABPBI/PBT Cast onto Grid.	19
17	Diffraction Pattern of ABPBI/PBT.	20
18	TEM Micrograph of Edges of Polymer Fibers in Specimen PBT (PPA).	20
19	Diffraction Pattern from Polymer Showing Good Crystallinity.	22

LIST OF ILLUSTRATIONS Continued

<u>Figure</u>		<u>Page</u>
20	Diffraction Pattern from Polymer Showing Ring Structure in Pattern, Indicating Low-Order Crystallinity.	22
21	(a) TEM Micrograph of TiC Powder Particles. (b) Diffraction Pattern from the Particles of (a).	23
22	Diffraction Pattern and Bright-Field Image of TiC Illustrating Results using the Spray-Nebulizer Technique.	24
23	Specimen Etched Using the Developed Etching Procedure. The material is Ti-5Al-2.5Sn + Ge, heated to 1975°F/15 min and water quenched.	31
24	Same Specimen as Fig. 23, Following Polishing and Etching Using Standard Kroll's Reagent.	32
25	Graphs Illustrating the Basis for Calculating Slope from an Experimental Curve.	41
26	Microstructures of Ti-5Al-2.5Sn PM Alloy. (a) As Received (b) After HIP'ing at 15 KSI, 1700°F, 1 hr.	50
27	Microstructures of Ti-5Al-2.5Sn-0.1Si (a) As Received (b) After HIP'ing.	51
28	Microstructures of Ti-5Al-2.5Sn-0.5Si (a) As Received (b) After HIP'ing.	52
29	Microstructures of Ti-5Al-2.5Sn-0.1Ge (a) As Received (b) After HIP'ing.	53
30	Microstructures of Ti-5Al-2.5Sn-0.5Ge (a) As Received (b) After HIP'ing.	54
31	Microstructures of Ti-5Al-2.5Sn-1.0Ge (a) As Received (b) After HIP'ing.	55
32	Profile Across the PCS Specimen Showing Variation in Concentration. The Sn exhibits a cyclic variation. The Al and Si variations are essentially random.	58
33	Profile Across the PCS Specimen Showing Ti Variation in Concentration. Large excursions are due to porosity in the specimen.	59

LIST OF ILLUSTRATIONS Continued

<u>Figure</u>		<u>Page</u>
34	Profile of Sum of Concentrations of Constituents in the Alloys. Note the 500× curve for No. 3; the flatness suggests that slow-magnification scans produce more uniform results.	61
35	Profile for 1.0 Ge Alloy Showing Variations in Al and Sn. Ge exhibits good uniformity across the specimen.	62
36	Profile for 1.0 Ti Alloy Showing Variations in Al and Sn. Ti exhibits good uniformity across the specimen.	63
37	Constituent Concentrations in Alloy No. 3 Normalized to Total Calculated Concentration. Excursions in Al, Sn, and Ti are evident.	64
38	Constituent Concentrations in Alloy No. 6 Normalized to Total Calculated Concentration. Excursions in Al, Sn, and Ti are evident.	65
39	Beta-Transus-Determination Results for HIP'd Base Alloy. (a-h) 1875°F to 2000°F in 25-Deg. Increments. Alpha-beta transus at 1850°F.	67
40	Microstructures of Ti-5Al-2.5Sn PM Alloy (a) As-Received, Aged 29 hr at 1000°F, (b) HIP'd Material, Same Age Conditions.	69
41	Microstructures of Ti-5Al-2.5Sn-0.1Si (a) As Received, Aged 29 hr at 1000°F, (b) HIP'd, Same Age Conditions.	70
42	Microstructures of Ti-5Al-2.5Sn-0.5Si (a) As Received, Aged 29 hr at 1000°F, (b) HIP'd, Aged 29 hr at 1000°F.	71
43	Microstructures of Ti-5Al-2.5Sn-0.1Ge (a) As Received, Aged 29 hr at 1000°F, (b) HIP'd, Same Age Conditions.	72
44	Microstructures of Ti-5Al-2.5Sn-0.5Ge (a) As Received, Aged 29 hr at 1000°F, (b) HIP'd Aged 29 hr at 1000°F.	73
45	Microstructures of Ti-5Al-2.5Sn-1.0Ge (a) As Received, Aged 29 hr at 1000°F, (b) HIP'd, Same Age Conditions.	74
46	Block Diagram of the Centorr Hot Press.	75
47	Block Diagram of the Brew Quench Furnace.	76

LIST OF ILLUSTRATIONS Continued

<u>Figure</u>		<u>Page</u>
48	Block Diagram of the Brew Vacuum Furnace.	77
49	Temperature Profile with Load Events (Hot Press).	81

SECTION I INTRODUCTION

Alloys of aluminum and titanium, nickel-base superalloys, nonmetallic materials, and composites are of major significance to the needs of the Air Force.

Research on high-strength aluminum alloys has now encompassed most of the compositions that can be made using standard melting and casting and work processes. There is considerable evidence that emerging powder technology will lead to alloys having improved combinations of strength, toughness, and stress-corrosion resistance, as compared to conventional alloys, and perhaps even improved fatigue properties. Associated with these new alloys, however, is a class of microstructures not existing in conventional alloys, and their role in controlling properties is not yet established.

One of the aims of the research of the AFWAL Materials Division is to examine microstructure/property relationships in order to identify any possible problems with the aluminum powder technology, and to examine the role of the various microstructural features in the new powder alloys in the light of their effects upon the mechanical and physical properties of fatigue-crack-growth rate, toughness, and stress-corrosion resistance.

Continuing efforts to improve titanium alloys, with respect to their performance, reliability, cost, and manufacturability, require a knowledge of the influence of metallurgical variables upon properties. The knowledge of processing and composition variables and their effects is necessary in order to obtain the desired properties with minimum cost. The AFWAL Materials Division's efforts to utilize relationships between microstructure and properties of titanium alloys to develop new alloys, alloys with minor alloying changes with respect to composition, and to improve mean values. The activities center around fatigue and fracture properties but, by necessity, includes other properties such as strength and

It is not currently possible to predict the mechanical properties of a material from its microstructure in a quantitative fashion. The ability to do so, however, would substantially reduce the amount of mechanical testing required to evaluate a material. Recognizing the increase in reliability and the cost savings that would result from the use of quantitative techniques, the Materials Laboratory has been active in the quantitative-metallography area in the past. The theme of the work has been the development of the techniques necessary for the recording of microstructural information in a form which can be handled by a computer and the development of the means for subsequently relating the microstructural information to the mechanical properties.

The quantitative-metallography effort has been concentrated mainly on titanium alloys since it is considered to be the most challenging area to pursue and the one where the need for quantitative techniques is greatest. However, the quantitative program was one of technique development and was directly related to the effort in microstructure/property relationships and not to other parts of this program.

The utilization of ceramics in turbine engines offers significant potential for increased efficiency and lower cost. Recognizing this, an Interagency Committee was formed for the Application of Ceramics to Turbine Engines was established by the Air Force to develop an interdependent program as a means of maximizing accomplishments. It was agreed that the Air Force would evaluate new materials developed by other organizations and also coordinate selection and characterization for the component programs of these organizations. The Materials Laboratory activity covers the area of material characterization and that area of mechanical behavior which is related to the application of ceramics to turbines.

Research has been placed by the Air Force on the durability of ceramic materials because of the rapidly increasing acquisition and maintenance costs of turbine engines and the burden to the Air Force in maintaining them to function at reasonable costs. One of the most significant results

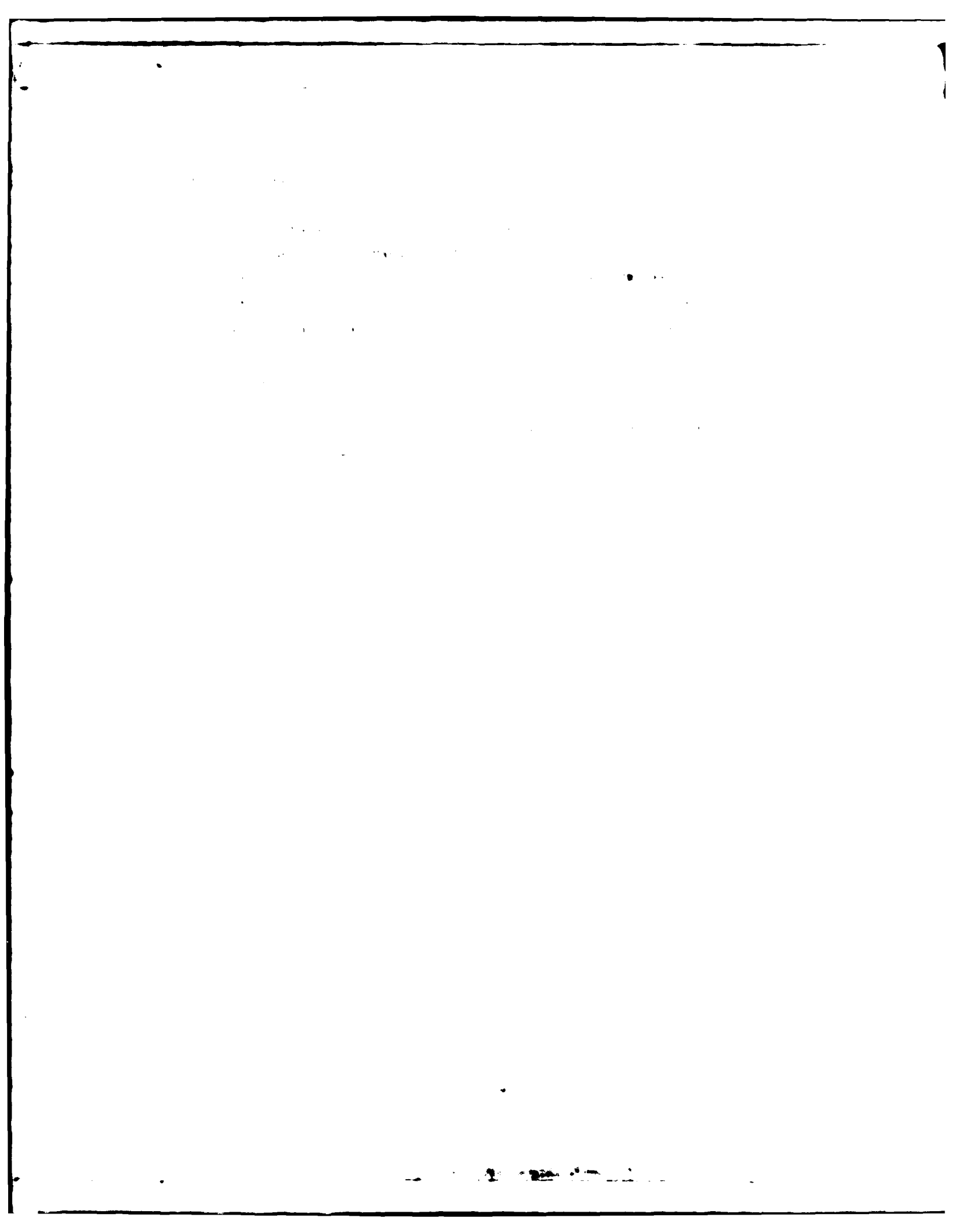
of the recognition of these problems was the introduction of the Damage Tolerant Design approach to new USAF airframes. Higher performance of advanced engines has produced a need to resort to more durable materials in engines. These problems have led to Materials Laboratory programs for development of improved techniques for predicting the service life of engine and airframe components and to investigations of means to control the corrosion, stress-corrosion, and corrosion-fatigue behavior of structural materials.

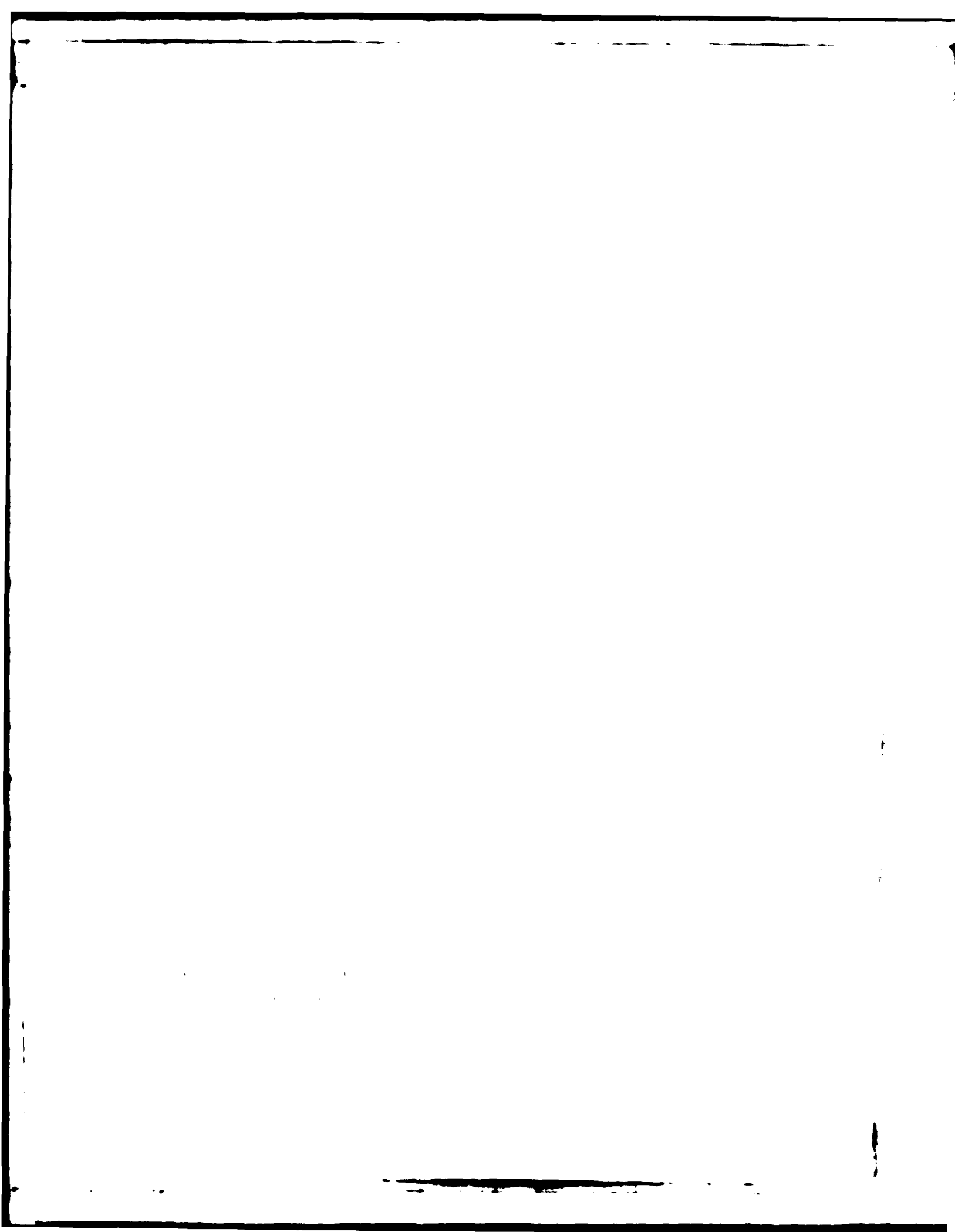
The program on microstructural characterization complemented work in the above areas being carried out within the AFWAL Materials Laboratory. Unique equipment and specialized investigative techniques available in this laboratory were used. The program provided the theoretical background required for effective accomplishment of objectives in the field of microstructural characterization of the inherently diverse exploratory probing nature of the program. To meet these needs effectively, the program was carried out at the AFWAL Materials Laboratory.

The overall objective of this program was to determine the microstructural characteristic of materials resulting from the various processes used in research and development programs. Microstructural characterization was integrated with on-going research and development of new materials in the AFWAL Materials Laboratory.

Techniques employed were optical metallography, quantitative metallography, and heat treatment. The required application of standard specimen preparation techniques of these methods.

Materials on which characterization was performed included nonmetals such as ceramics, carbon-fiber composites, and Alloys included those of aluminum, titanium, and Boron-titanium-silicon composites and titanium alloys.





as a furnace, together with related equipment (e.g., thermocouples, thermocouple sensing, measuring and controlling devices). A small shop was also maintained for fabricating needed parts.

RESEARCH AND MANAGEMENT OF FACILITIES

Because of the wide variety of materials characterized and the integrated nature of the efforts to be accomplished, it was necessary to organize the work so that results were produced on a timely basis in a coordinated manner by the personnel conducting the research. Control of the work was exercised by the project manager via work orders.

Requests for work were submitted on a work order describing the work to be done. The work was assigned to the appropriate person responsible for accomplishing the work, who then performed the work and reported results directly to the initiator. Schedules were maintained for the work.

Time accounting was accomplished by means of time sheets showing hours expended on each project. These sheets were used to estimate the time used by each project. This information was then compared with the time estimates submitted by various Materials Laboratory (WIP's) for each project. This was done for determining whether a requester's estimate was reasonable. Authorized WIP's were those who were authorized to conduct materials research and had the necessary controls. Without such controls, research could be conducted in a haphazard manner, leading to gross overruns.

Research, structure, adequate control and documentation were achieved. The research was organized so that work areas were settled through the use of a system of control, reference to the SOW, and use of a system of control to ensure that the objectives were met.

Section 3
RESEARCH ACCOMPLISHED

The research accomplished during the program was reported in detail in the form of papers published or presented, in quarterly and annual reports, and through discussions with appropriate engineers and scientists with whom the work was integrated.

The publications authored or co-authored by SRI personnel are listed below. The accomplishments reported in these papers were related to studies of Al alloys, Ti alloys, superalloys, nonmetallics, and ceramics. Copies of the papers are available from the authors.

PRESENTATIONS AND PUBLICATIONS

1. "Preparation of Single Aluminum Powders for TEM Observation,"
R. Santner and R. Omlor, TMS-ATME Fall Meeting, St. Louis, MO,
October 1978.
2. "Crack Initiation in Ti-6Al-4V Castings," D. Evlon and M. B. Stroppe,
J. Mater. Sci., 14, (1979).
3. "Microstructural Characterization of Titanium Alloy Powders," R. E. Omlor,
J. C. Eckert, E. C. Bacon, D. Evlon, and E. H. Froes, ASM-IMS Meeting,
June 1979.
4. "Formation of a Secondary Fatigue Crack in CI 91 Aluminum Powder,
Alloy Powder," W. M. Griffith, M. M. Cook, and R. E. Omlor, EMSA-MAS
Meeting, August 1979.
5. "Kinetics of the Growth of Minimum Set of Standards,"
J. C. Eckert and M. B. Stroppe, Microbeam Analysis Society,
San Antonio, TX, August 1979.

6. "Morphological and Microstructural Evaluation of Various Titanium Alloy Powders," D. Eylon, R. E. Omlor, R. J. Bacon, and F. H. Froes, AIME Symposium on Ti Powder Metallurgy, Las Vegas, NV, February 1980.
7. "Microstructure Property in Cold Pressed and Sintered Elemental Ti-6Al-4V Powder Compacts," Y. Mahajan, D. Eylon, R. Bacon, and F. H. Froes, AIME Symposium on Ti Powder Metallurgy, Las Vegas, NV, February 1980.
8. "Thin Foil Preparation of Prealloyed Metal Powders," L. E. Matson and R. E. Omlor, Second Annual International Conference on Liquid Solidification Processing Principles and Technology, Reston, VA, March 1980.
9. "Advanced Titanium Alloy Development via Powder Metallurgy," A. G. Jackson, J. Moteff, and F. H. Froes, TMS-AIME Symposium on Ti PM, Las Vegas, NV, February 1980.
10. "Dispersion Hardening of the Ti-5Al-2.5Sn Alloy Using a Powder Metallurgy Approach," A. G. Jackson, J. Moteff, and F. H. Froes, Fourth International Ti Conference, Kyoto, Japan, May 1980, and published in The Science Technology Application of Ti, Metallurgical Society of AIME, 1980.
11. "Selected-Area Diffraction Ring Patterns in Al-Zn-Mg Powders," J. Santner and R. E. Omlor, J. Mat. Sci. 15, 784 (1980).

HIGHLIGHTS OF SPECIFIC MATERIALS-CHARACTERIZATION-FACILITIES ACTIVITIES

Brief descriptions of representative research efforts will now be presented for electron-optics, optical metallography, quantitative metallography, and special projects. Only the highlights are presented here since detailed reports have been submitted separately.

Electron-Optics

Transmission Electron Microscopy

In the Al-alloy research, a technique for preparing thin foils for TEM was studied and modified. This technique allows preparation of a foil from material adjacent to a fracture surface; this permits study of the modes of damage accumulation. During the course of this study, a secondary fatigue crack in a 6191 aluminum powder product was isolated.

The fracture surface of a fatigue crack-growth specimen was removed using a diamond cut-off saw and ground until only traces of the original roughness remained. The opposite side of the sample was ground until an 8-mil thickness was attained. Using a cupped punch, 1/3-in. disks were removed from the sample. The disks were carefully ground (on the side opposite the fracture surface only) to a 3-mil thickness. The sample was then electropolished in a double-jet polisher until both sides were shiny (60 sec.). One side of the polisher was marked off to protect the fracture surface from further attack, and electropolishing continued on the side opposite the fracture surface until perforation occurred.

Polishing solution: 20% HNO_3

Current density: 60 V, 25 mA

Temperature: -35°C

Polishing unit: Twin-Jet Fischione.

Samples representing dehydrided and hydrided Ti-6-4 were examined. The hydrided specimens were very brittle, and the macrosample required a special masking-polishing technique before electropolishing could be performed using standard techniques. The specimen was cut at a thickness which prevented breaking, 10-15 mil, and then five 3-mm discs were marked off using a TENKI acid-resistant tape and microstop. This bulk sample was then polished, and fairly uniform 3-mm discs were produced--still at a thickness of 10-15 mil. These discs were hand polished down to a thickness

of 3-5 mil and then electropolished using standard polishing techniques. More than 200 micrographs have been taken of this type of specimen. Some examples are shown in Figs. 1-4.

The Philips 300 electron microscope was used in a series of tests on Ti 6-4 + H with the hot-stage attachment. The specimen was tested at several temperatures for fixed periods of time, the final temperature being 350°C for 20 min. Examples of the work are Fig. 5-6 which show the same area subjected to various heat treatments.

In a continuing program on AF 115 and AF 2-1DA superalloys, a method was required for producing high-quality, high-magnification micrographs of the special features of superalloy fatigue and fracture surfaces. SEM photomicrographs were taken on the ETEC of areas of interest (see Fig. 7) for reference purposes. These areas were then replicated using standard replicating techniques. A special copper grid was then used for the replica. This grid (Martiform grid made in England) has the alphabet imprinted on it (see Fig. 8). Using optical microscopy, the replica was then placed in the grid and the location of the area of interest marked, according to the alphabet. In this way, the area of interest could be located easily in the TEM. Figure 9 is an SEM micrograph of a pore and its cracks, and Fig. 10 is a TEM replica showing the pore and its cracks. Other examples of TEM replication are shown in Figs. 11-14. As illustrated by these figures, this method produced good results for AF 2-1DA and AF 115 superalloys.

Nonmetallic Materials. A program involving blended polymer samples was initiated. Since this material is very sensitive to the electron beam (radiation damage, heat, etc.), extensive sample-preparation techniques (including microtomy) were required. In the first stage of this program, blends of PBT and AB-PBI polymers were cast from solutions onto stainless-steel grids. Figures 15-17 show single crystals isolated using this method



10,000x
Figure 1. Ti-6-4 Undeformed Dehydrogenated Specimen Showing Slip.



49,500x
Figure 2. Ti-6-4 Undeformed Dehydrogenated Specimen Showing Dislocation Network.



26,000x
Figure 3. Bright Field of Ti-6-4 95H
Platelets.



26,500x
Figure 4. Dark Field of Ti-6-4. Same
area as Fig. 3.



Figure 5a. Initial Condition of Ti-6Al
4V + H Specimen.



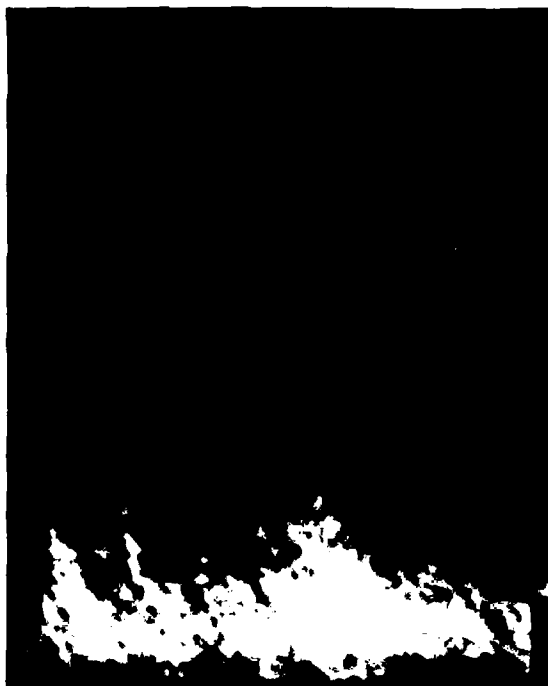
10 min. 200°C
Figure 5b. Effect of Heating at 200°C
upon Dislocations Present in
the Hydride.



5 min.

350°C

Figure 6a. Initial Condition of Ti-6Al-4V + H Specimen.



20 min.

350°C

Figure 6b. Effect of Heating at 350°C upon Dislocations Present in the Hydride.

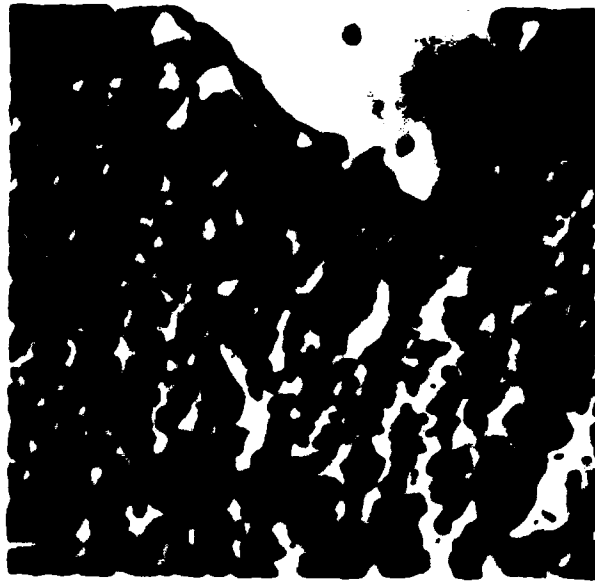


Figure 7. SEM Photomicrograph Taken on the EEP.

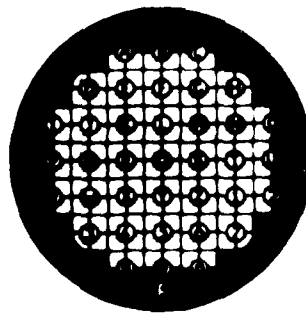


Figure 8. Lettered Grid Used to Locate Areas of a Specimen.

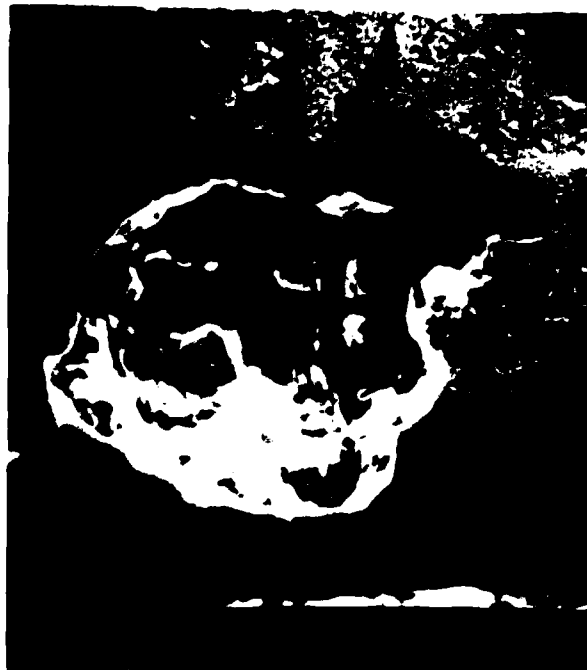


Figure 9. SEM Micrograph of a Pore and Its Cracks.

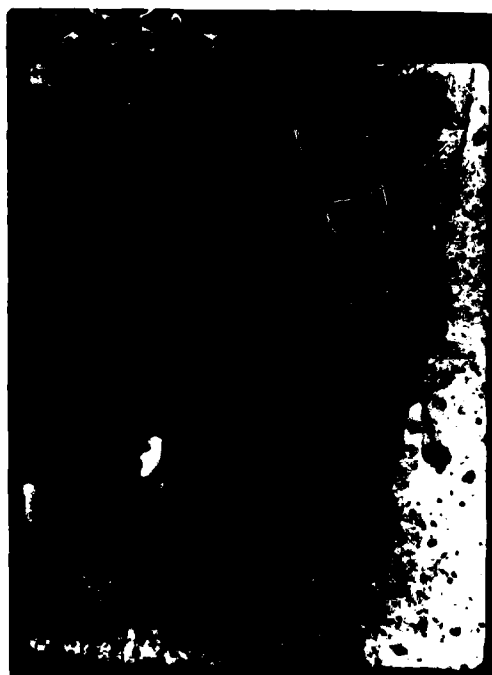


Figure 10. TEM Replica Showing a Pore and Its Cracks.



38,500x

Figure 11. Large Carbide Particle.



31,000x

Figure 12. Shear γ' Near the Pore.



Figure 12. Major Crack and Parallel Slip Lines

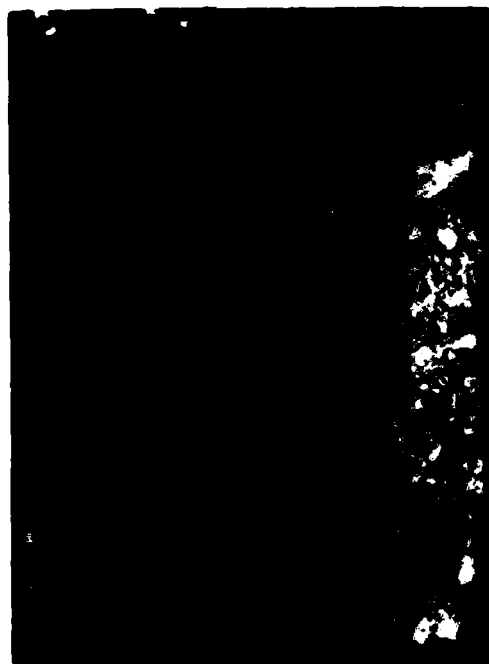
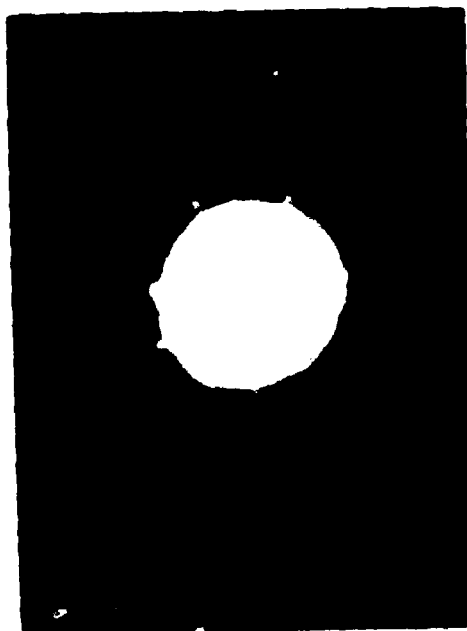
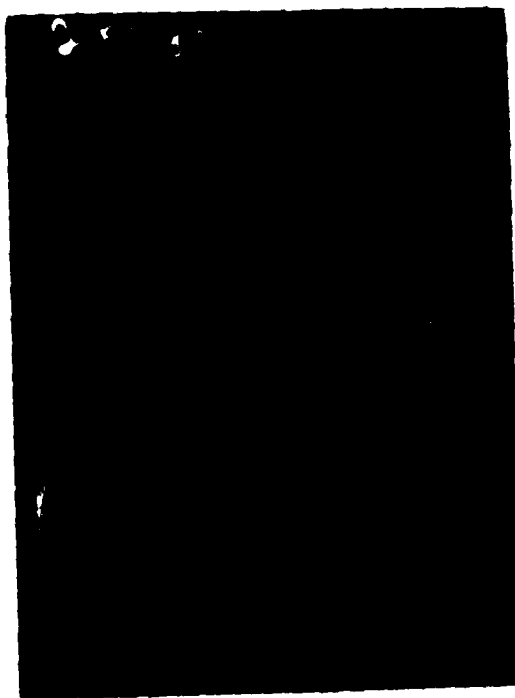


Figure 13. Crack From Pore to Edge and Sheared off



20/60

100% (100% ABRA) 100% (100% ABRA)



20/60

100% (100% ABRA) 100% (100% ABRA)

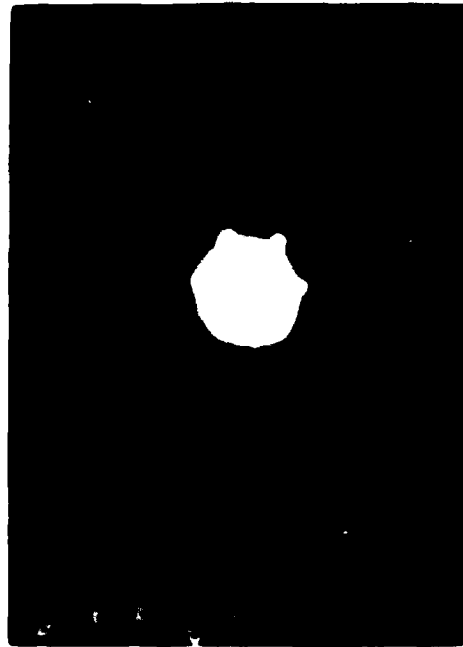


Figure 18. (a) Micrograph of a single crystal of PMMA (PPMA).



Figure 19. (b) Micrograph of a single crystal of PMMA (PPMA) at 34,000x magnification.

ing their diffraction patterns. Various other methods of sample preparation were explored and microtome samples prepared. For example, a 1% PBI solution in MSA bottled in Na_2O was prepared; the film was washed, then fractured, and placed in the microscope for observation. 100% PBI cast films MSA was heat treated at 600°C for 15 min. in N_2 . Low illumination of the film was also required. Figure 18 shows the edges of typical polymer fractures. Figures 19 and 20 illustrate the types of diffraction patterns that were obtained with these polymers.

Analysis of the required special dispersion techniques in order to separate the powder particles for examination. The TiC powders were ultrasonically dispersed and sprayed on carbon-coated grids. With this method particle morphology could be examined. Figure 21a shows TiC No. 12, and its electron diffraction pattern is shown in Fig. 21b. The purpose of this research was to determine particle size and shape and to obtain electron-diffraction patterns. Figure 22 illustrates the results of this technique on a TiC powder.

Electron Microscopy

Particle examination was conducted on various Ti powders produced by various firms in Europe. The purpose of this effort was to identify the microstructure, porosity, and contaminant level present in the powders. Various other powders were characterized. The procedure used was to coat, fracture, and etch the samples to determine the microstructure and impurity content, e.g., tungsten contamination from the electrodes used to manufacture the powder. Powders were also examined directly by SEM. Fractures of the powders, produced by various processes such as HIP'ing or cold-chamber sintering, were evaluated for microstructure.

The examination site of primarily consisted of determination of fracture initiation sites and identification of any unusual features present at the site, e.g., pores, particles, foreign elements, and compounds. Materials examined included experimental alloys of aluminum (CT91), nickel-base alloys (IN-73), composites (fiberglass), and nonmetallics (polymer fractures).

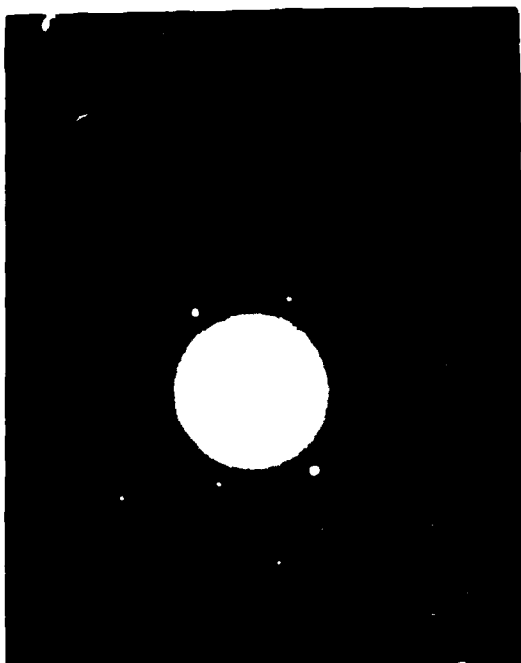


Figure 19. Diffraction Pattern from Polymer Showing Good Crystallinity.

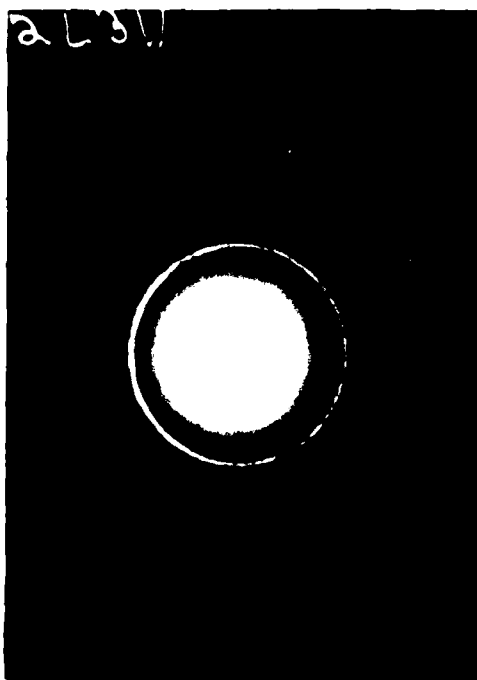
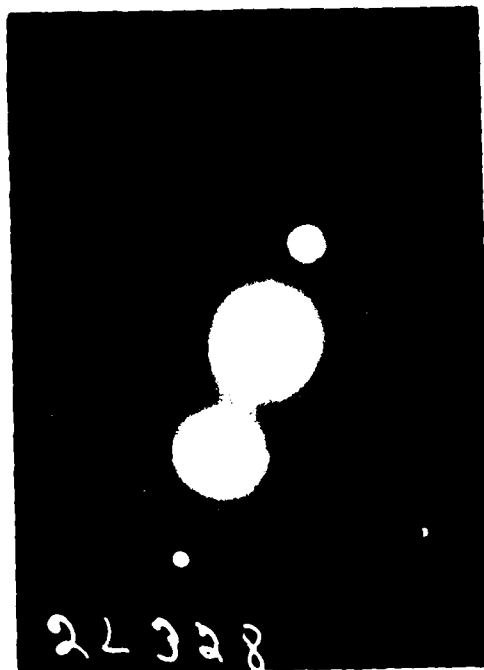


Figure 20. Diffraction Pattern from Polymer Showing Ring Structure in Pattern, Indicating Low-Order Crystallinity.

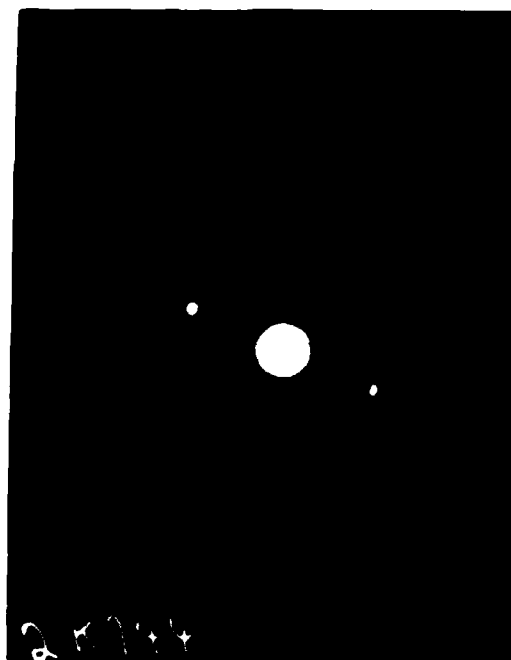


(a)



(b)

Figure 21. (a) TEM Micrograph of TiC Powder Particles.
(b) Diffraction Pattern from the Particles
of (a).



(a)



(b)

17,000x

Figure 22. Diffraction Pattern and Bright-Field Image of Hc Illustrating Results Using the Spray-Nebulizer Technique.

Electron-Probe Microanalysis

Significant progress was made in efforts to provide quantitative analyses routinely. Early in the program the ZAF program from NBS was obtained, debugged, and made operational on the CDC 6600 system. In 1979 a small computer system (Apple II) was acquired to allow faster turn-around in completing computations. The ZAF program was translated from FORTRAN to BASIC, debugged, and put into operation on the Apple II system. The use of the Apple II is now routine for analyses of from two to nine elements. Modifications and improvements to the BASIC program have been made which simplify its use and facilitate changes in output formats or increases in scope.

As part of the research effort, a short course was presented on quantitative analysis of EPMA data. The goal of the course was to provide sufficient background information on EPMA calculation methods to enable EPMA users to assess their results correctly and to familiarize them with the NBS FRAME IV program being used. The lectures stressed the physical processes involved and the equations used to describe these processes. Examples of research performed are presented below.

Al Alloys. Samples of aluminum powder-metal alloy were examined in an attempt to determine the cause of low strength. Large particles were observed in each sample, with Specimen #235 having fewer and smaller particles than #108. A sample of good material showed no such particles. The larger and more blocky the particles, the lower the magnesium content. In the following tables, both weight percent and atomic percent are given.

Sample #235

Element	Test 1		Test 2		Test 3		Average	
	Wt%	At%	Wt%	At%	Wt%	At%	Wt%	At%
Mg	2.2	2.0	2.0	2.4	0.8	1.1	1.7	2.1
Al	73.1	82.7	80.6	87.5	68.3	82.3	74.0	84.2
Cr	0.3	0.2	0.3	0.2	0.1	0.0	0.2	0.1
Fe	2.3	1.3	1.5	0.8	2.7	1.6	2.2	1.2
Co	20.9	10.8	13.3	06.6	24.0	13.3	19.4	10.2
Cu	2.4	1.1	2.3	1.1	1.8	0.9	2.2	1.0
Zn	2.4	11.1	3.3	1.5	1.6	0.8	2.4	1.1

Sample #108

Element	Test 1		Test 2		Test 3		Average	
	Wt%	At%	Wt%	At%	Wt%	At%	Wt%	At%
Mg	0.1	0.0	1.3	1.8	0.0	0.0	0.5	0.6
Al	65.0	82.1	65.5	80.8	65.8	81.8	65.4	81.6
Cr	0.1	0.0	0.0	0.0	0.0	0.0	0.0	0.0
Fe	2.6	1.6	3.1	1.8	2.6	1.6	2.7	1.7
Co	26.1	15.1	24.4	13.8	26.9	15.3	25.8	14.7
Cu	1.3	0.7	2.0	1.0	1.4	0.7	1.6	0.8
Zn	1.0	0.5	1.5	0.8	1.1	0.6	1.2	0.6

An aluminum powder-metal alloy was examined to determine the chemistry of rod-shaped precipitates in the 0.0%Co sample. Also a 0.4%Co alloy was examined to determine whether rod-shaped precipitates were present. The particles are too small for quantitative analysis. The relative X-ray counts obtained by EDS are given on the following page. Notice that the ppts. are high in iron and copper, possibly Al_7Cu_2Fe .

0.4X Cobalt Sample

	Mg	Al	Fe	Co	Cu	Zn
Round particle	2201	112452	606	4198	644	1512
Round particle	2503	110894	906	5480	546	1401
1.5 x.5 rod	1929	111307	911	6800	592	1176
Matrix	2396	130023	0	0	498	2316

Ni-Base Alloys. Extensive quantitative analysis was performed on two IN100 specimens having different grain sizes to determine whether a difference exists in composition. The difference in chemistry between the matrix and the gamma prime was compared. The sample identified as IDX has finer grains than the sample D N Radial. The gamma prime is similar in both, but the matrix differs. The analysis is as follows:

D N Radial Specimen, Matrix, Spot Analysis

Element	1	2	3	4	Avg.
Al	4.76	4.49	4.65	4.79	4.67
Ti	4.52	4.55	4.51	4.57	4.54
V	1.20	1.20	1.16	1.19	1.19
Cr	14.76	14.80	14.34	14.54	14.61
Co	19.97	20.28	19.55	19.82	19.91
Ni	51.93	51.51	51.80	52.01	51.81
Mo	3.89	3.80	4.04	4.30	4.01
Total	101.02	100.63	100.06	101.21	100. 74

Steels. Fracture surfaces in 4340 steel were examined for fatigue in air and fatigue in an SO₂ environment. The air sample had a very rough surface with much secondary cracking. Ductile tear was noted even in the fatigue area whenever a stringer was found, and there were many in the short-transverse specimen. Several fields of round inclusions were noted. The SO₂ sample had a rough surface also, but fewer stringers were observed and there was much secondary cracking. This was a very confusing fatigue area, and no fatigue lines were observed. Much of the surface was covered with contamination which may have masked the fatigue striations.

Nonmetallics. Quantitative analysis of copper-sulfide films on various substrates posed several problems which made analysis impractical. The electron beam, even at only 5 kV, caused some of the samples to bubble. This led to the speculation that some of the sulfur was being removed during analysis. By using a fast scan at TV rates and 5000× magnification, the bubbling was greatly reduced although the estimated energy being dissipated was still about 500,000 W per square meter. It was felt that none of the samples was infinitely thick to the electron beam, which means that the substrate is contributing to the total yield of X-rays.

Averages of three scans of copper and sulfur counts were tabulated for all specimens and compared with conductivity data which were supplied with the specimens. Three tests per specimen are ordinarily insufficient for determination of the exact ratio with a high degree of reliability. However, the other factors mentioned above make this a reasonable number.

SEM photos of the surface of each specimen were also taken at two different magnifications. Most of the samples have particles which are high in copper. Sulfur from the As₂S₃ substrates contributes to the total count and, therefore, the calculated percentages for As and S are too high. In general, ratios from similar substrates should be compared. Lower copper content seems to produce better conductivity. If thicker layers can be deposited (about 2 μ), this analysis could be accomplished on the probe.

Ceramics. Si_3N_4 which had been oxidized for 36 hr at 1300°C was characterized for concentration profiles of Ca, Mg, and W as a function of depth from the surface to the interior of the specimen. Tungsten was found as small particles distributed throughout the specimen. Mg increased toward the center but seemed to be constant after the first 100 to 150 μ . However, Mg was high in the outside layer. Ca concentration was very low in the specimen, but there was a layer of Ca-rich material around the outside of the specimen. Although oxygen could not be detected, it might have been present in modest concentrations.

Metallography and Photo Labs

Research on preparation of specimens for examination of the microstructure was accomplished on a wide variety of materials. These included Al alloys, P/M alloys, superalloys, steels, fiber-reinforced alloys, and graphite fibers. Each type of material requires the use of a different technique or extension of a technique to reveal unusual specimen features. Preparation consists of cutting, grinding, polishing, mounting, etching, and heat treating as well as documenting the macrostructure and microstructure.

In several cases the influence of etching and polishing techniques upon the Al alloys and upon the superalloys was systematically examined. Such examination was required because the standard techniques did not produce a suitable finish. The microstructure was obscured by polishing or etching.

Specimen preparation of B-III Ti, Ti powders, Ni-base superalloys, and various other Ti alloys was accomplished. Also a great deal of time was spent on developing a color metallographic technique for the identification of phases in hydrogenated Ti alloys. Reports of this work were presented at the 1978 IMS meeting.

Specimen-Preparation Technique. Metallographic preparation of materials often requires the use of special etchants and/or techniques to reveal the microstructure, particularly when new alloys are involved, as in the

Metallurgical characterization studies being conducted on PM Ti-5Al-2.5Sn. This material required prolonged final polishing and many polish/etch cycles for proper pore development and for removal of disturbed etch. Unfortunately, past etching techniques resulted in staining that could not fully be removed by final polishing. Hence, the final product was poor. After numerous attempts to correct this condition, the following procedure was developed to minimize staining in these alloys:

- 1) Swab etch using 40 ml glycerol, 10 ml nitric acid, 2 ml hydrochloric acid, and 1 ml hydrofluoric acid.
- 2) Rinse immediately in flowing hot water.
- 3) Quickly dry using air blast.
- 4) Immediately swab specimen with 20% sulfuric acid solution.
- 5) Rinse in water, neutralize with sodium-carbonate solution, rinse again, and dry.

The technique is applicable to other Ti PM alloys as well. The potential for forming nitroglycerin compounds was thoroughly examined. To form this compound anhydrous-glycerol is required. The glycerol used in the etch is 95% pure, the remainder being water. Thus, there is no significant chance that any explosive compound will be formed. Caution in use of this etch and prompt disposal, however, must be exercised. The effectiveness of this technique is illustrated in Figs. 23-24.

In addition to usual task assignments during the period, of particular interest was a failure analysis performed on a hydraulic pump conducted in conjunction with the Fluids, Lubricants, and Elastomers Branch. Steel used in the fabrication of the plate was very dirty. In the weakened condition, it was not able to withstand the stress conditions relative to heat treatment and, as a result, cracked in the thin section adjacent to the hole.



Figure 23. Specimen Etched Using the Developed Etching Procedure. The material is Ti-5Al-2.5Sn + Ge, heated to 1975°F/15 min and water quenched.



Figure 24. Same Specimen as Fig.23 , Following Polishing and Etching Using Standard Kroll's Reagent.

In the following tables, summaries of the work accomplished in the Metal Laboratory and photo labs during the course of the program are presented. In the miscellaneous category, includes processing of micrographs, full film processing, and processing of other sizes of prints.

SUMMARY OF WORK FLOW IN METALLOGRAPHY LAB

May 1977 - August 1980

Month	Specimens		
	1977-78	1978-79	1979-80
May - July	696	798	269
August - October	233	902	210
November - January	397	679	193
February - April	735	289	406
May - August	-	-	430

SUMMARY OF WORK FLOW IN THE PHOTO LABS

1977 - 1978

	4 x 5	8 x 10	Slides	Misc.	Color	
	2168	433	192	84		
	1454	72	88	456		
	1004	319	100	53	10	
	3324	293	545	273	23	
Total	7950	1117	925	866	33	10891

Average of 42 items/day

PHOTO LAB SUMMARY
May 1978 - April 1979

	1 - 4	5 - 8	neg	Vol	color	Misc	Total
May	626	45	29	22	14	--	736
Jun	473	88	58	10	0	--	629
Jul	969	101	21	0	0	--	1,091
Aug	550	316	18	21	4	167	1,066
Sep	1,103	91	17	43	1	116	1,361
Oct	581	19	13	14	0	170	787
Nov	572	166	21	24	29	0	792
Dec	84	143	22	8	0	14	269
Jan	607	69	3	16	14	0	709
Feb	267	328	0	0	2	183	699
Mar	530	24	44	34	23	114	765
Apr	1,000	44	8	0	0	183	1,235
TOTAL	8,534	1,788	263	241	103	1,000	12,929

THE FEDERAL BUREAU OF INVESTIGATION

NAME	ADDRESS	CITY	STATE	ZIP	DATE
ALFRED E. BROWN	1234 5th Ave.	New York	NY	10001	1-15-64
JOHN D. SMITH	4567 12th St.	Chicago	IL	60601	1-15-64
MARY K. JONES	7890 3rd St.	Los Angeles	CA	90001	1-15-64
ROBERT L. GARCIA	2101 7th Ave.	San Francisco	CA	94101	1-15-64
CHARLES W. HILL	3456 9th St.	Philadelphia	PA	19101	1-15-64
ELIZABETH A. WHITE	5678 11th St.	Boston	MA	02101	1-15-64
WILLIAM F. BLACK	8901 13th St.	Seattle	WA	98101	1-15-64
BARBARA J. GREEN	1012 15th St.	Portland	OR	97201	1-15-64
DAVID R. MILLER	1314 17th St.	San Diego	CA	92101	1-15-64
JANE M. WATSON	1616 19th St.	Denver	CO	80201	1-15-64
JOHN P. ROY	1918 21st St.	Phoenix	AZ	85001	1-15-64
MICHAEL S. LEE	2220 23rd St.	San Jose	CA	95101	1-15-64
SARAH L. HARRIS	2522 25th St.	San Antonio	TX	78201	1-15-64
THOMAS H. KING	2824 27th St.	Fort Worth	TX	76101	1-15-64
ANGELA B. WALKER	3126 29th St.	Memphis	TN	38101	1-15-64
CHRISTOPHER D. YOUNG	3428 31st St.	Indianapolis	IN	46201	1-15-64
DEBORAH K. ADAMS	3730 33rd St.	Columbus	OH	43201	1-15-64
ERNEST J. NELSON	4032 35th St.	San Jose	CA	95101	1-15-64
FRANCIS M. STEVENSON	4334 37th St.	San Jose	CA	95101	1-15-64
GRACE A. HUGHES	4636 39th St.	San Jose	CA	95101	1-15-64
HOWARD R. FLEMING	4938 41st St.	San Jose	CA	95101	1-15-64
IRIS L. BAKER	5240 43rd St.	San Jose	CA	95101	1-15-64
JAMES E. SCOTT	5542 45th St.	San Jose	CA	95101	1-15-64
KATHLEEN M. GREENE	5844 47th St.	San Jose	CA	95101	1-15-64
LAWRENCE P. COLLINS	6146 49th St.	San Jose	CA	95101	1-15-64
MARGARET S. PERKINS	6448 51st St.	San Jose	CA	95101	1-15-64
NATHANIEL J. ROBERTS	6750 53rd St.	San Jose	CA	95101	1-15-64
OLIVIA K. TURNER	7052 55th St.	San Jose	CA	95101	1-15-64
PETER M. PHILLIPS	7354 57th St.	San Jose	CA	95101	1-15-64
RENEE A. CAMPBELL	7656 59th St.	San Jose	CA	95101	1-15-64
STEPHEN L. EVANS	7958 61st St.	San Jose	CA	95101	1-15-64
TIMOTHY R. ROSS	8260 63rd St.	San Jose	CA	95101	1-15-64
URSULA M. HENDRICKS	8562 65th St.	San Jose	CA	95101	1-15-64
VICTOR J. COOPER	8864 67th St.	San Jose	CA	95101	1-15-64
WILLIAM F. REED	9166 69th St.	San Jose	CA	95101	1-15-64
XENIA K. BARNES	9468 71st St.	San Jose	CA	95101	1-15-64
YOUNG L. FOSTER	9770 73rd St.	San Jose	CA	95101	1-15-64
ZACHARY M. GIBSON	10072 75th St.	San Jose	CA	95101	1-15-64

Calculation of cooling rates from the sizes yielded acceptable times on the order of 10^{-2} to 10^{-1} sec. Credibility in the measurement, however, requires a standard to allow estimation of standard deviations expected with this type of measurement.

Ring Measurements. A group of Ti-6-4 rings was received for measurement of the area. The accuracy was required to be as high as could be realistically obtained, i.e., $\pm 1/2\%$ of diameter.

Previous measurements using the epidiastroscope on the OM-20 system had yielded results which were somewhat operator dependent. An extensive series of tests was conducted using reference areas in order to determine the accuracy expected in these types of measurements on the OM-20.

The tests showed that an accuracy of $\pm 4\%$ could be easily obtained on an average. In order to obtain more accurate readings, corrections to the image would be required. The largest contributor to error was barrel distortion in the lenses of the image orthicon. The larger the area of the live frame occupied, the larger the false enlargement of the area being measured. A detailed determination of this distortion was not attempted because of time limitations. Instead, a different procedure was adopted.

A standard area of 1.000 ± 0.000 in. was machined. Using this, together with the ring, a photograph was taken of each ring/standard area combination. Measurement of the ring area and the standard area was then made using the digitizer in the area-measurement mode. Accuracies attained in this way were $\pm 0.7\%$ diameter (1.4% area). While this method required that someone physically measure each area as well as photograph the rings, the high accuracy of results justified the use of this approach.

size distribution of the pores in Superalloys. Information on pore size in powdered-metal superalloys was required for an alloy which had been subjected to forging. Three sides were examined in order to determine whether the direction of forging had affected the pore size. The OM 720 was used to determine the pore sizes by means of the classifier-collector module. Using this module, absolute size of a given feature was measured by taking the interval of picture-point size accepted and converting this picture-point interval into units of a linear measurement in microns.

On several occasions, on a number of occasions, an image analysis of a microstructure from the OM 720 was requested. Usually the required analysis was an image attraction or a size distribution. In responding to these requests, it became clear that the operation and limitations of the OM 720 were not fully appreciated. To assist the engineers in finding the best use of the unit needed, a thorough review of the machine was made from a functional point of view.

Since the instrument was in need of a thorough overhaul by a serviceman, evaluation of the utility of the instrument was risky. Problems identified were:

1. Lenses on the epiliascope needed factory adjustment for focus.
2. The TV camera required factory recalibration and tuning.
3. IC Mod No. 2 overloaded frequently and the picture-point count produced was too large. A new board was required in the module.
4. No manual was available for the 2-P autodetector, making use of this module dependent upon exploring the effects of each switch and control.

5. The operating manual for the entire system was vague and poorly written. Development of procedures directly applicable to metals was required.
6. Room atmosphere was dirty; temperature was poorly controlled; the air conditioning was not usable.
7. The Reichert microscope required alignment on one of the optical axes. This required a serviceman or access to special tools and jigs for alignment.
8. Barrel distortion in the epidiascope lenses was significant for accuracies better than $\pm 2\%$.
9. Stage drive in the x direction required repair. The stage tended to stick during motor-controlled movement.
10. Stage alignment with the optical axis of the microscope was poor.

Most of these problems could be dealt with during service calls. The air-conditioning problems would be processed through the building monitor and base personnel.

Since these system difficulties could not be cleared up, the potential of the QM in relation to research required was determined to be minimal, and the unit was turned in.

Digitizer. The HP digitizer available in MLLN was used for some problems not tractable on the QM. In particular, if a photograph of the surface of interest could be made and an area or distance measurement was desired, then the digitizer was the simplest route to accomplishing this work. Intrinsic accuracy of measurement on the digitizer is ± 0.01 in. Closed areas, individual lengths, curve length, and several other geometrical measurements can be made using this device. Since a HP 9820 calculator is part of this system, as well as a plotter, further refinement of the data can be done immediately or as part of the measurement itself.

microdensitometer. An optical microdensitometer available in the lab was used for this purpose. An attempt was made to use this instrument for measuring the optical transmission on SEM micrographs. The effort was only partially successful, due to differences in contrast between the dendrite arm and its background. The measurement of the area, but the amount of effort required as compared to that of a manual intercept measurement by hand was so excessive in time, that no further efforts were made to use the microdensitometer. The instrument was transferred to a different branch.

Graphics Tablet. In order to accomplish quantitative-metallography tasks--intercept, particle-distribution analysis--a graphics-tablet accessory was obtained for use with the APPLE II system. This tablet has the capability of digitizing data entered by use of an electronic pen and a photoelectric sensor pad. Software for general use of the tablet was obtained with the accessory; but specific programs for calculating areas, perimeters, and particle count must be written. An area-measurement program was written which prints each area based on an approximation of the area as a disc. A second program which prints coordinates of a point was also written. More complex versions which will store the data, convert to absolute area, and calculate volume fractions are possible through modifications to existing programs.

The continuous-curve-slope program allows one to enter reference lengths and scale factors for the experimental graph (see Fig. 25a). The basis of the slope calculation is to first generate an array of (x,v) points continuously by running the pen smoothly over the curve (Fig. 25b). This array is then divided into equal increments in the x direction. The v values in each increment are added to find an average value of v. This value and the value of x associated with the interval then become the coordinates of a computer-generated curve (Fig. 25c). The larger the number of increments, the closer the generated curve approximates the experimental curve. However, because of limitations in the plot on the printer, the practical values for the number of increments should be in the range 40-60. The maximum number of intervals usable is set at 99.

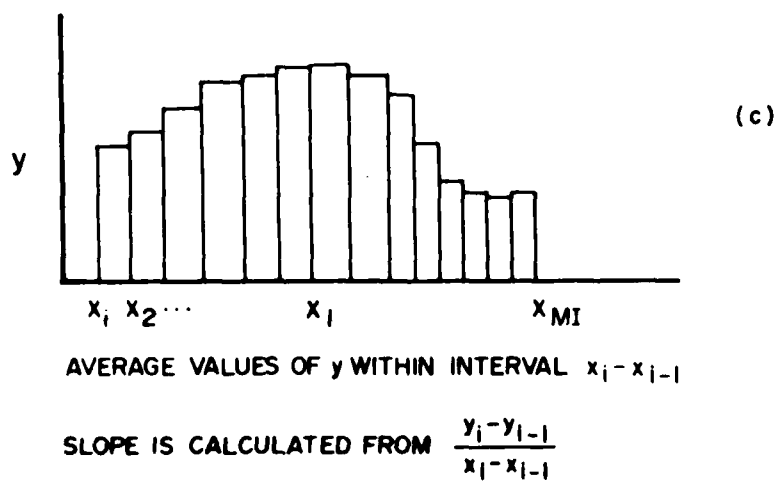
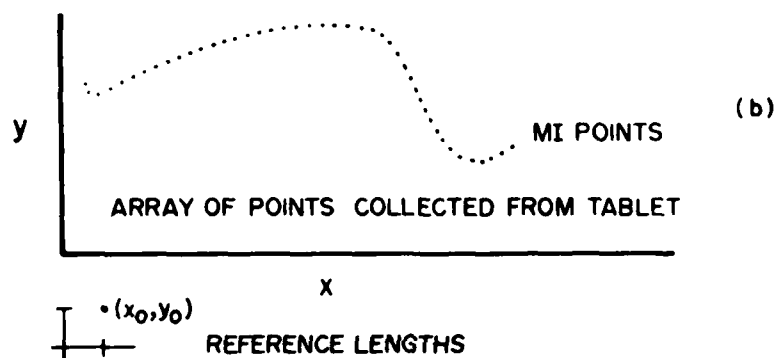
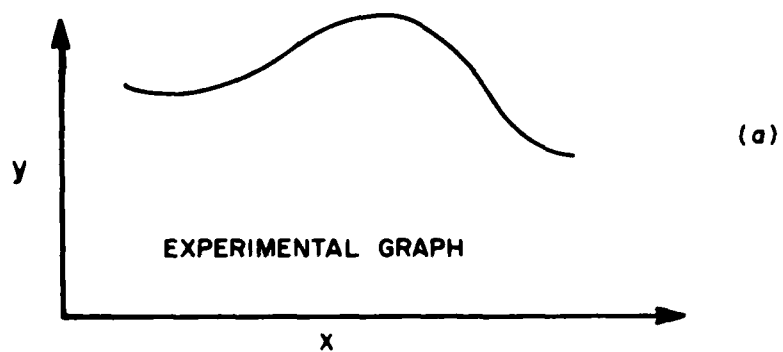


Figure 2. Graphs Illustrating the Basis for Calculating Slope from an Experimental Curve.

The procedure is as follows:

Use graphics table disk (has slope written on it). Turn on printer.

Put disk in drive

Press reset

Type 6, then hold down CTRL key and press P

Press return key

Wait for APPLE logo to come on screen

Press ESC key

Press Q

Press return

Type RUN CONTINUOUS. CURVE. SLOPE

Enter x factor

Enter v factor

Take pen and locate reference square

Press pen down at lower left corner of square

Wait for beep

Press pen down on upper right corner of square

Scale factors will be printed out

Take pen and locate starting point on curve

Hold it down and move pen until at end of curve

Lift pen up

Place pen at top of tablet, press down once

The rest of program runs, finishing with plot of slope curve.

10-12	Dimension statements setting upper limits on subscripted variables
20	Control statement
30	Command to bypass subroutines
200-280	Subroutine to obtain a set of x, y values from the tablet
300	Clears the tablet
310-320	Inputs of unit factor (x, y) on graph (number of units/cm)
330	-
340	Command to generate (x, y) points
350	First set of values for (x_0, y_0) for reference scale
360	Time delay to allow operator time to use the pen
370	-
380	Command to generate (x_1, y_1) values
390	Second set of values for (x, y) for reference scale
400	Calculate difference ($x_1 - x_0, y_1 - y_0$)
410	Calculate scale factors:

therefore $xs = \frac{XR}{XD}$ $ys = \frac{YR}{YD}$ $XS, YS \equiv$ scale factor
 $XR, YR \equiv$ unit distance on
the tablet
 $XD, YD \equiv$ graph reference scale

```

415      Turn on the printer
420      -
430      Turn off the printer
440-500  Routine to generate (x,y) points continuously
470      check to stop collecting data.
510      Increment MI since it is too large by 1 because of 490
515      Turn printer on
520      Enter the number of increments into which the curve is to be
          divided for generating points on the curve. The purpose is to
          create a curve that has NX points generated from the MI set of
          points obtained in section 440-500.

```

622-641 This section, through the sort subroutine at 800-1100, finds
 the maximum and minimum value of the MI points in the x array.

 642 XI = interval = $\frac{(\text{max}-\text{min})}{\text{number of increments}}$
 643 XX = Max value of x
 644 XN = Min value of x
 645 NX = Number of intervals
 646 Definition of values needed in plot routine
 647-648 This section finds the max and min values of the MI points in
 the x array.
 649 YY = Max value of y
 650 YN = Min value of y
 651-652 Initializing statements for variables
 653-656 XC(0) = incremented value of X for the NX increments
 657-660 calculate the average value of y in the x increment LK-1 to LK
 661-662 summing these values of x in the MI points which are
 current value of x. Start at LL = 1, compare values in
 x array to be sure that the value is less than the current
 average value of Y(LK). If it is, then take the value of y
 and add it to all other values of y found so far.
 663 calculate the average value of y in the interval increment

$$YAV(LK) = \frac{\text{sum of Values}}{\text{Number of X's Summed}} = \text{zero value of y}$$

 664
 665 Flag on value of NL. This ends the loop for values > NX
 666 Increment NL by 1
 667 Set the LL to start at last point of previous interval
 668 Zero YY
 669 Loop to seek next value of LK (x increment)
 670 Keep the X value
 671 Define XZ
 672-679 calculate length of x axis
 700 Command to business subroutines
 800-1100 sort subroutine

1200-1350 Slope calculation subroutine

Since differences in points are to be found, the number of points to be calculated will be one less than entered at line 520. A second point is lost at the end also because of taking differences. Hence, the total number of points is $NK-2$.

1250 Calculate slope

$S(JS) = y \text{ difference} / x \text{ difference}$

2000-3080 Plot routine

2002 Calculate slope

2015 Print values of interval number NX

(on printer) x value

y value

2130 Print number of points to be plotted N

2200 Print coordinates of points

2235 Print array of values

2300 Print values of (x,y) where axes intersect

Data Analysis. To assist in satisfying the data-analysis objective of the scope of the work, a number of computer programs have been prepared for use with the data-acquisition system. These programs are written in BASIC and are readily transferrable to FORTRAN for use on the CDC 6600 terminals, if required.

Currently the following are available:

GAUSS - calculates and plots on CRT various Gaussian distributions.

FRAME EDS - ZAF correction program using EDS data.

FRAME WDS MOD - ZAF correction program using WDS data.

FRAME ANGLE - ZAF correction program using WDS or EDS data as function of angle.

LEAST SQUARES - calculates least-squares fit to set of data.

SECOND ORDER FIT - calculates a fit to a specific second-order equation.

LN1 VS (E-EK) N - calculates least-squares fit to equation

$$\ln \frac{I_1}{I_0} = n \ln (E-E_K)$$

LN1 VS LNE - calculates least-squares fit to $\ln I$ vs $\ln E$

RATIOS - calculates ratios of peak data for given elements. All combinations are included.

THOR COUNT - calculates equivalent K-line counts using curve-fit parameters.

RATIO LEAST SQUARES - same as above but fits calculated data to a curve by least-squares method.

MOD RATIO LSO - modification to above.

NTH ORDER REGRESSION - calculates least-squares curve for nth order equation.

MULT. LIN. REGRESSION - calculates linear fit for multiple variable set of data.

FLA - calculates backscatter coefficients for use with alloy data.

TRUNC - truncates output of calculated quantity to desired length.

In addition to these mathematical routines, the system will process character arrays. Several programs have been written for tracking hours charged, titles of papers on file, sorting of data, or lists by size or alphabetical order.

Special Projects

Research on Ti Powders and PM Products. Detailed characterization was performed on a number of Ti alloy powders. The thrust of the effort was to characterize the powders in terms of morphology, phase, impurity type, chemistry, dislocation structure, and thermal stability. Because of the magnitude of the effort, it was divided into two parts. The first dealt with conventional alloy powders and the second specifically with Ti-Al-2.5Sn with additions of Si and Ge. The first part is discussed in the TEM and the SEM subsections, and the second part is explained in this subsection.

It is necessary to characterize Ti P/M alloys with dispersions and second phases present because of the changes induced in the mechanical properties by such inclusions. Since this is a complex problem, a simple α -alloy was chosen for detailed characterization in order to obtain a better understanding of the role of dispersions such as Si and Ge. Si is a potent strengthener in Ti alloys when used in very small amounts, while very little is known about Ge in Ti alloys. Also Ge has a higher solubility than Si and is expected to be less mobile which would lead to more desirable properties than those yielded by Si in Ti alloys.

The initial focus of this effort was to characterize a specific Ti alloy as an example of the influence of partially soluble dispersoids upon Ti P/M alloys.

Literature-based data on Ti-Si alloys were gathered; and button melts of Ti, Ti-Si, and Ti-Ge alloys were prepared.

Six types of specimens produced by the Gould elemental-blend method were received. These were cold compacted at 15 tons and sintered at 2300°F for 4 hr. Sections from each were made. Specimens of each type were sent to Kelsey-Hayes for HIP'ing at 15 KSI and 1700°F for 2 hr. Extrusions of conventional alloys were made and sections were cut from one extrusion.

The P/M alloys prepared were as follows:

1. Base (Ti-5 Al-2.5 Sn)
2. Base + 0.1 Si
3. Base + 0.5 Si
4. Base + 0.1 Ge
5. Base + 0.5 Ge
6. Base + 1.0 Ge

Early results were partially reported in two papers prepared for presentation (see list of publications). Details of these papers not included because of space limitations are presented below. Efforts included analysis of porosity, thermal etching, aging experiments, and analysis of one extruded alloy.

Porosity in each of the alloys was measured using optical micrographs. Since the Quantimet 720 system was not functioning, the Zeiss particle analyzer was used with 8 × 10 enlargements of the original micrographs. Three sets of photos were used. The first set (original: 50×) proved to be useful for testing the technique, but did not provide sufficient resolution of the pores to be of value. The next two sets of micrographs were taken at 200× which, when enlarged to 8 × 10 prints, allowed reliable analysis of much more detail.

Corrections for magnification were made which translate the measured diameters to actual diameters in the specimen. The lower limit of measurement was about 4 μ , which was determined by the resolution of the Zeiss analyzer.

Based upon these counts, plots of count vs. diameter were made to determine the type of distribution for the pores. The curves suggest that the distributions are exponential. To evaluate this observation, techniques described by Underwood¹ were used in which the experimental distribution is set equal to a product of two functions. The first is a probability function which takes into account the randomness of the slice through the specimen. The second is the theoretical distribution function for the pores. The data were analyzed using Gaussian, constant, and exponential (or log-normal) type distributions. The best fit in terms of general shape was produced using the exponential-type distribution function.

Using the frequency data, area fractions for the pores were calculated and plotted. Comparison of as-received to HIP'd specimens clearly shows the reduction in area fraction and mean pore diameter achieved with the HIP'ing conditions used.

Microstructures of the as-received and HIP'd material were determined. Comparison of as-received alloys (CCS) with HIP'd materials (CCSH) is shown in Figs. 26-31. The as-received material generally exhibited α -laths with some indication of a second phase at the lath boundaries.

The HIP'd material shows a grain structure together with the original α -laths. This grain structure has sharp boundaries, and the grains tend to surround several α -laths. Definition of the laths is reduced with a broadening of boundaries. The large pores tend to situate themselves at lath boundaries. Small pores exhibit no preference for location in the laths or the large grains. Boundaries pass through pores for both types of pores. Thermal-etch experiments ($T = 540^{\circ}\text{C}$ for 4 hr in vacuum) did not clearly reveal the microstructure, although some changes were evidently related to loss of definition of lath boundaries.

TEM foils of several samples were made by mechanically thinning a slice to about 0.010 in. and then jet thinning to perforation. Results were marginal. Porosity of the material caused thinning to occur unevenly, making TEM observation of the structures difficult. The tendency was to etch near the material in the pore area, leaving very small thin edges around the pores. These could be penetrated by the TEM electron beam. However, the area between the pores which was the bulk of the foil was too electron dense to permit observation of the details of the material.

In those areas which could be observed, pores which had not been etched, i.e., which were in the interior, were observed to contain material different from the bulk. STEM analysis of these pores, carried out at Hitachi and JEOL Instrument Laboratories, showed the presence of Fe and Cl. He β was detected on the edge of opened pores as well as in the form of 0.1 μ particles.

Probe analysis of the specimens established the values of the concentrations of elements present. Results suggested that the specimens are homogeneous down to tens of microns.



(a)



(b)

Figure 26. Microstructures of 11-5Al-2.5Sn PM Alloy. (a) As Received, (b) After HIP'ing at 15 KSI, 1700°F, 1 hr.



(a)



(b)

Figure 27. Microstructures of Ti-6Al-4V alloy (a) As received, (b) After HIP'ing.

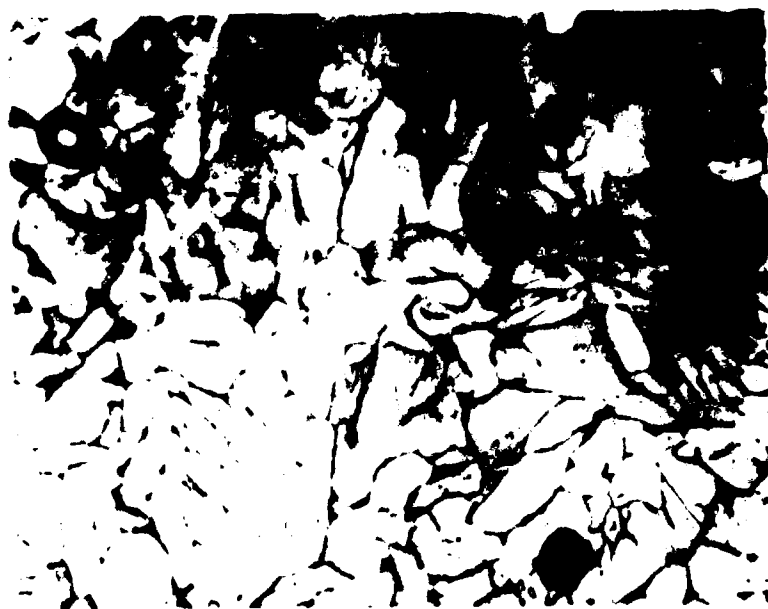


(a)



(b)

Figure 28. Microstructures of Ti-5Al-2.5Sn-0.58Zr (a) As Received, (b) After HIP'ing.



(a)

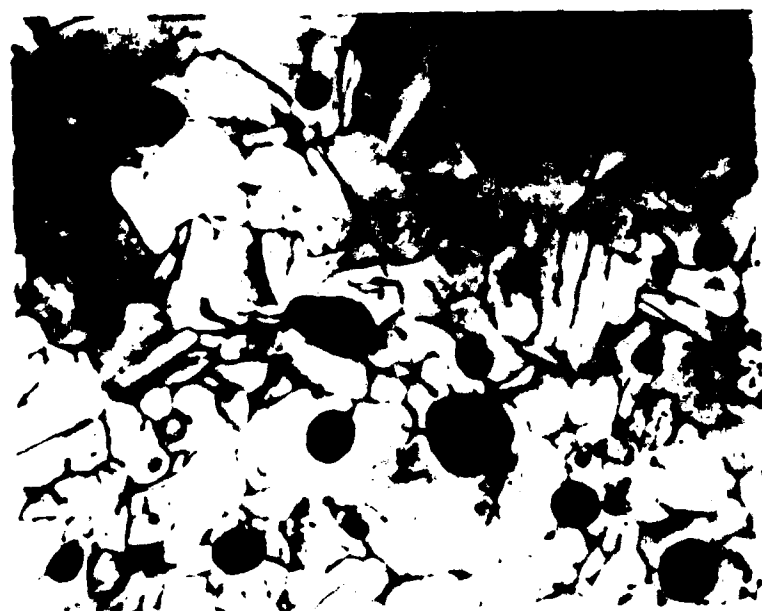


(b)

Figure 29. Microstructures of Ti-5Al-2.5Sn-0.1Ge (a) As Received, (b) After HIP'ing.



(b)

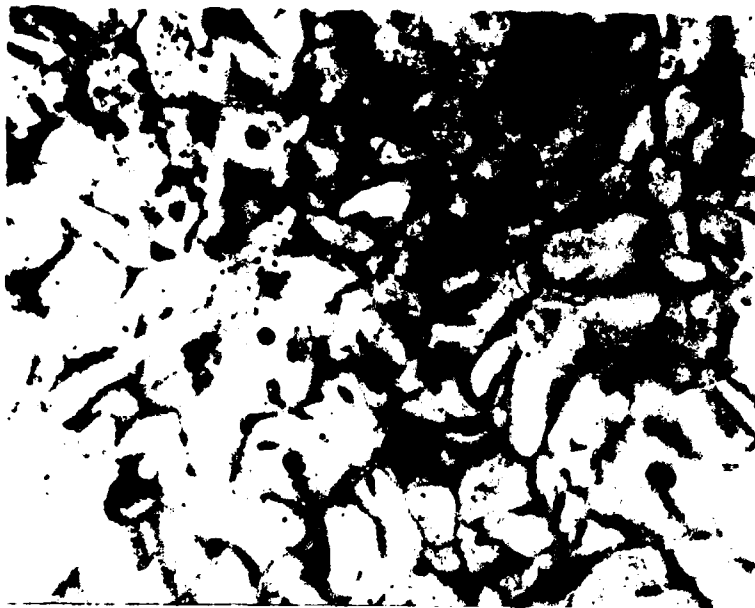


(a)

Figure 30. Microstructures of Ti-5Al-2.5Sn-0.5Ce (a) As Received, (b) After HIP'ing.



(a)



(b)

Figure 31. Microstructures of Ti-5Al-2.5Sn-1.0 Ce (a) As Received, (b) After HIP'ing.

problems due to porosity of the specimens may arise since the possibility exists of analyzing on a spot where a large pore is just beneath the surface. Care was taken to avoid this situation by examining regions where no larger pores were evident and by examining several spots. All data were taken using a reduced scanning mode at a magnification of 2000x. This approach reduced contamination in the area scanned.

Second phases present in several specimens were examined to determine qualitatively any differences in composition as compared to the interior of the α -laths. Differences in counts were found for Al and Sn. Ti, Ge, or Si counts were essentially unchanged. The table below shows raw WDS count data obtained from the base plus 1.0 Ge alloy. The differences between the interior and the lath boundary are small but definitely real for the as-received specimen. For the HIP'd material, the difference in Al is suspect, but the difference in the Sn count is significant.

BASE PLUS 1.0 w/o Ge, AS RECEIVED

	<u>Interior</u>	<u>Lath Boundary</u>
Al	3700	3100
Sn	1325	1698
Ti	298704	297455
Ge	815	849

(Counts Time = 50 sec)

BASE PLUS 1.0 w/o Ge, HIP'd

Al	770	780
Sn	3510	3820
Ge	2100	2100
Ti	298704	297455

Homogeneity studies were performed using the microprobe on three of the as-received alloys. As a result of work reported by Boyer, *et al.*,² at the 1980 Las Vegas AIME Meeting, a detailed probe examination of three of the as-received alloys was made. The problem in conducting such analyses is the possibility of instrumental errors which could be interpreted as real variations in concentration. Consequently, most of the effort in collecting data was expended in identifying possible instrumental errors which could significantly contribute to spread in the measured concentration of an element.

The approach taken was to scan the beam in a reduced mode at high magnification (5000 \times), taking data at fixed spots along the x direction. The counts were converted to concentrations, and plots for each element were made.

Variations in concentration for the base + 0.5 Si alloy are shown in the plots in Figs. 32-33. One expects some variation in the concentrations because of the statistical nature of the counting process and the approximations used in calculating the concentrations. Ordinarily these are on the order of 5 to 10% relative error. Thus, it is not surprising to observe that the concentrations vary across the specimen. The question to be answered is whether there is a pattern to the variation or whether the range of variation is unusual.

The Al concentration appears to be relatively flat across the specimen. There is no obvious trend. Si exhibits a possible trend to lower values across the specimen, but the results are not clear cut in this case. Sn, on the other hand, shows a distinctive oscillation in concentration and a trend to higher values at one end of the specimen. There appears to be a cyclic variation. The Ti plot, while showing what appears to be large fluctuations, is generally flat. The spread in values is within the 5 to 10% range, as expected.

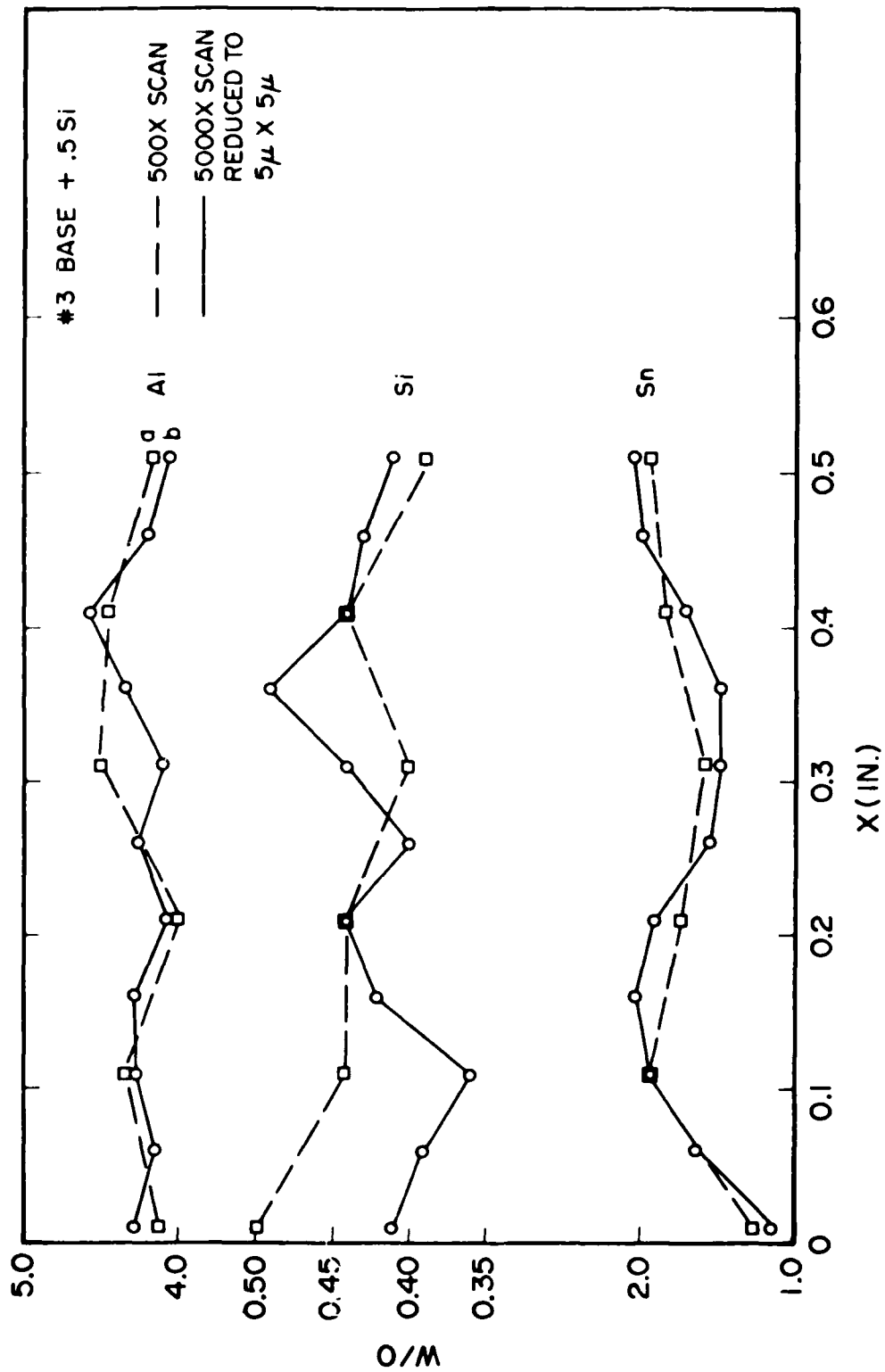


Figure 32. Profile across the PCS Specimen Showing Variation in Concentration. The Sn exhibits a cyclic variation. The Al and Si variations are essentially random.

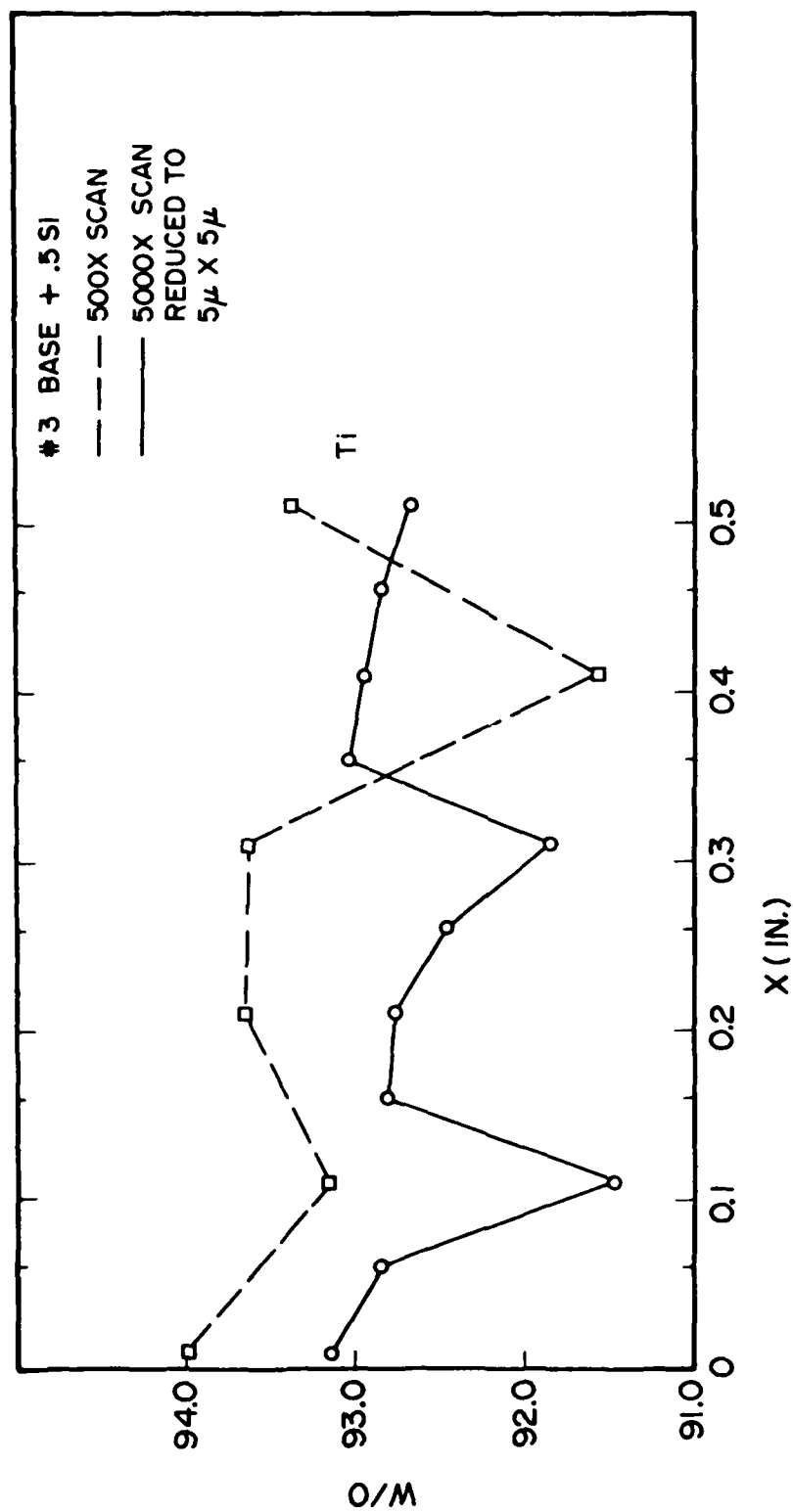


Figure 33. Profile Across the PCS Specimen Showing Ti Variation in Concentration. Large excursions are due to porosity in the specimen.

Figure 34 is a plot of the total concentrations for Specimen Nos. 3 and 6 (Si and Ge alloys). The data indicate that overall, the sum of all the concentrations is relatively constant to a few weight percent, as expected.

The results for the base + 1.0 Ge are illustrated in Figs. 34-36. Variation in Al across the specimen is within expected values, and the general curve is flat. Similar conclusions apply to the Ge and the Ti concentrations. As with Specimen No. 3, the Sn values exhibit a trend to higher values at one end of the specimen.

The data were normalized to the calculated total in each case and for each spot on the specimen in an effort to reduce the effects of fluctuations due to calculational approximations, which result in the total concentrations summing to values other than 100%. For the data this is an acceptable procedure since it is certain that contributions from other elements are very small. The results of the normalization are shown in Figs. 37-38. Conclusions from the unnormalized data still hold. The only element to exhibit strong variations is Sn. The plot accentuates the cyclic nature of the variation. The rather smooth sinusoidal variation may indicate that the instrument is varying--not the concentration.

These results have helped to define the variations in concentration which are present, but the results are still open to question. It seems clear that Al is relatively uniform across the specimen and that Ge and Ti are also within expectations. Si may be inhomogeneously in solution since there is a possible trend to linear variation across the specimen. The case of Sn is unusual in that the variations appear to be sinusoidal or cyclic in nature. It is possible that the probe beam was placed on Sn-rich phases when the data were taken at one point and not on Sn-rich phases at other points. This could explain the scatter in the data from the other elements and Sn. The difficulty with this interpretation is that the smooth cyclic variation as one moves across the specimen surface is not what is expected if the beam is randomly placed on Sn-rich and then Sn-deficient phases. One would expect a wide range of values randomly placed on the plot of concentration versus distance.

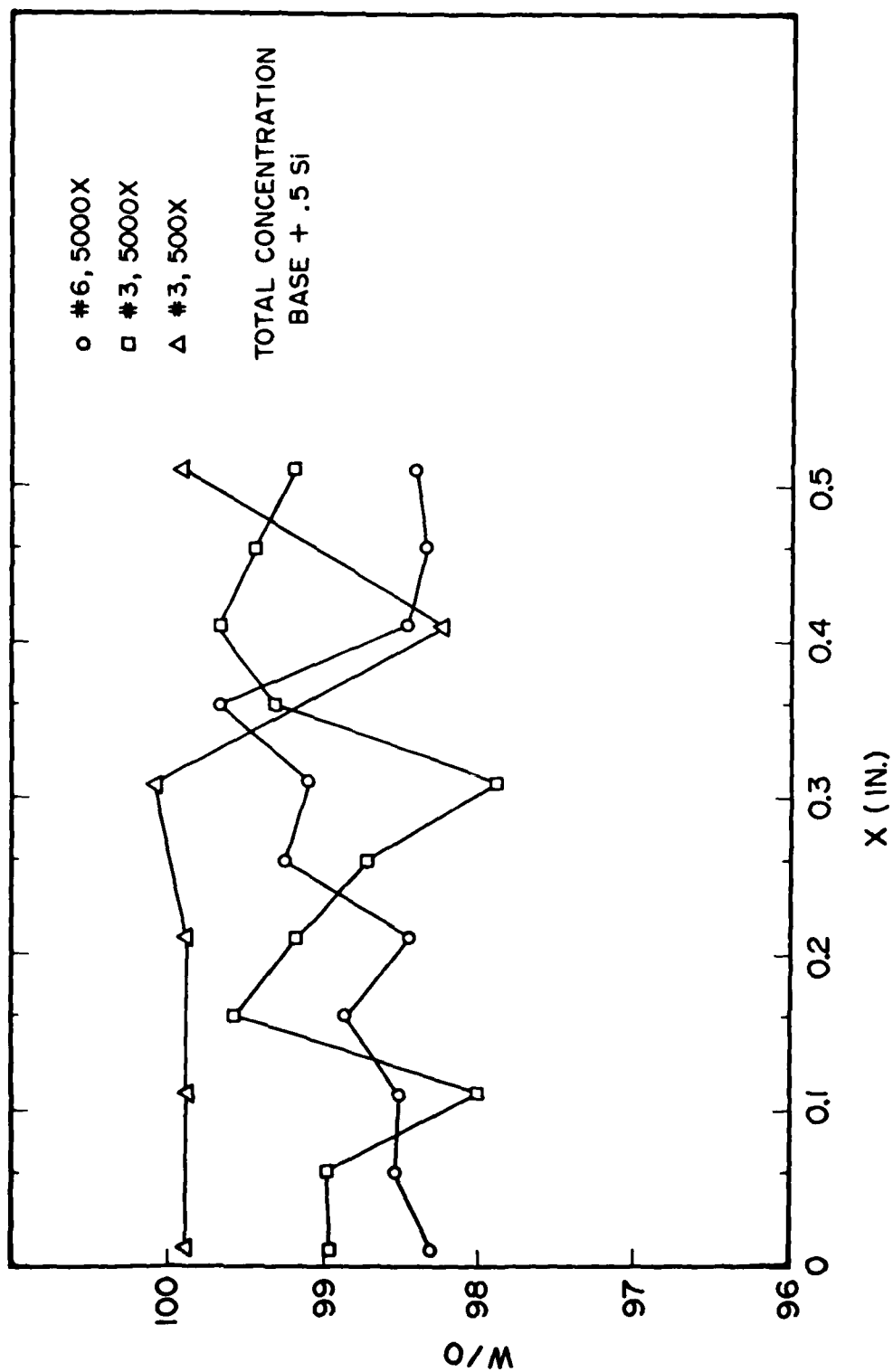


Figure 34. Profile of Sum of Concentrations of Constituents in the Alloys. Note the 500. curve for No. 3; the flatness suggests that slow-magnification scans produce more uniform results.

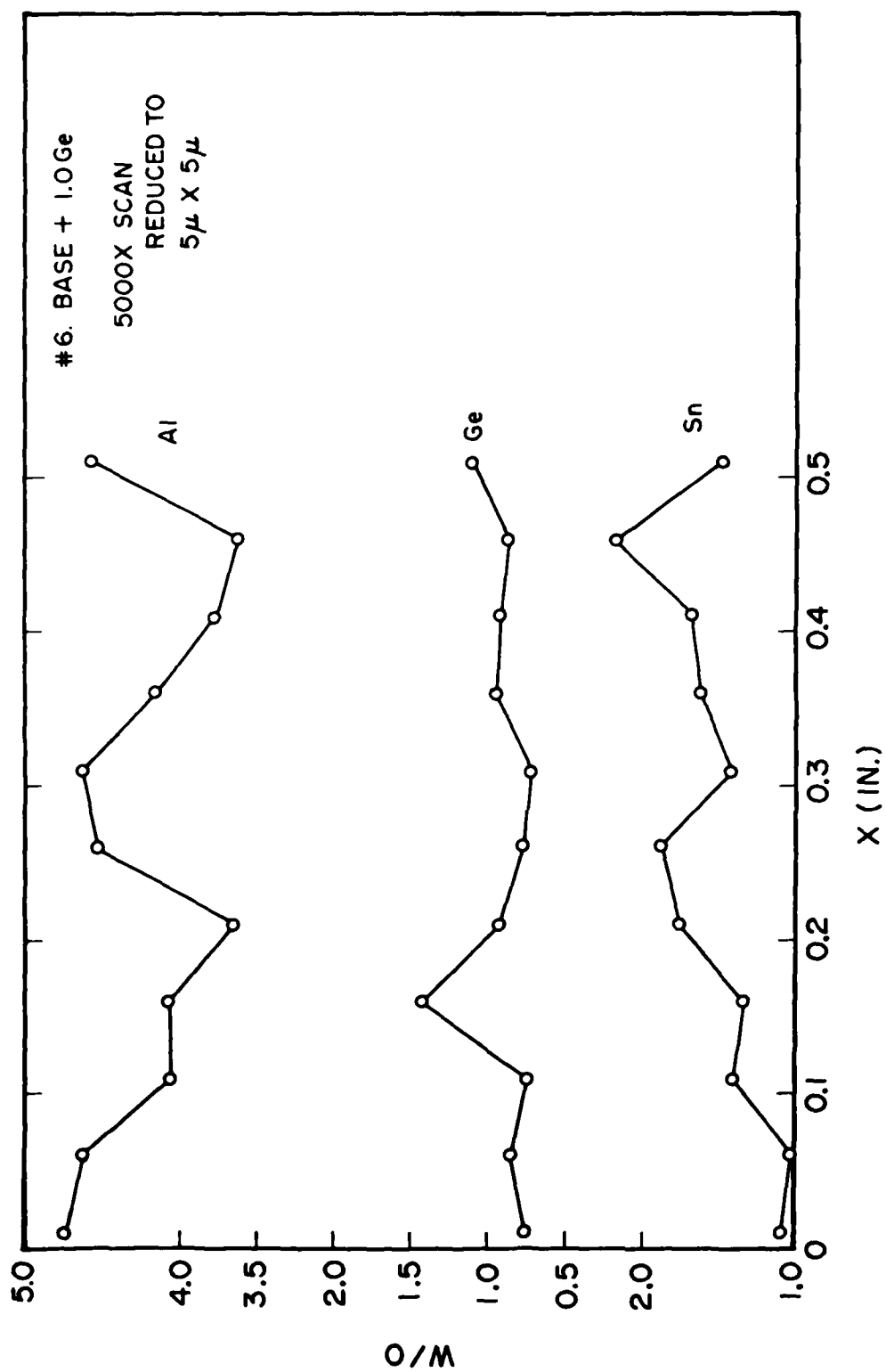


Figure 35. Profile for 1.0 Ge Alloy Showing Variations in Al and Sn. Ge exhibits good uniformity across the specimen.

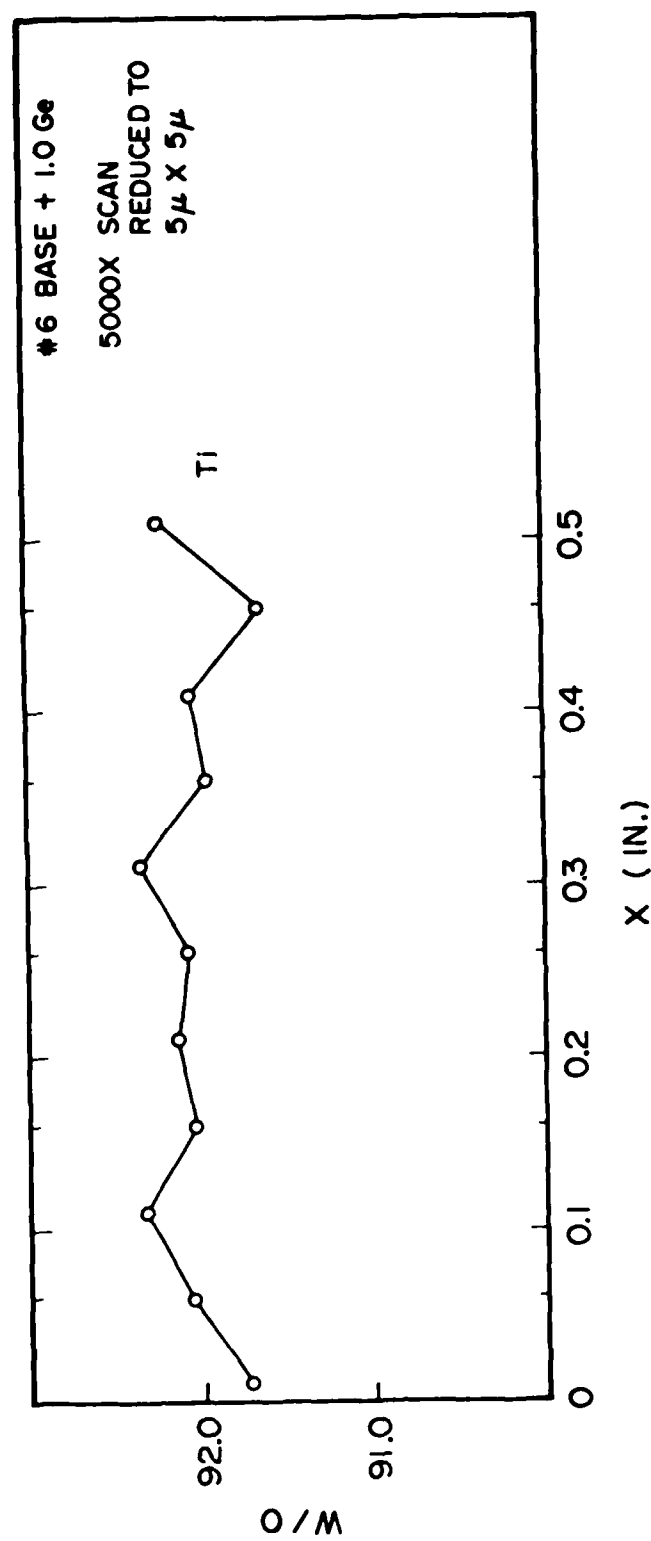


Figure 36. Profile for 1.0 Ti Alloy Showing Variations in Al and Sn. Ti exhibits good uniformity across the specimen.

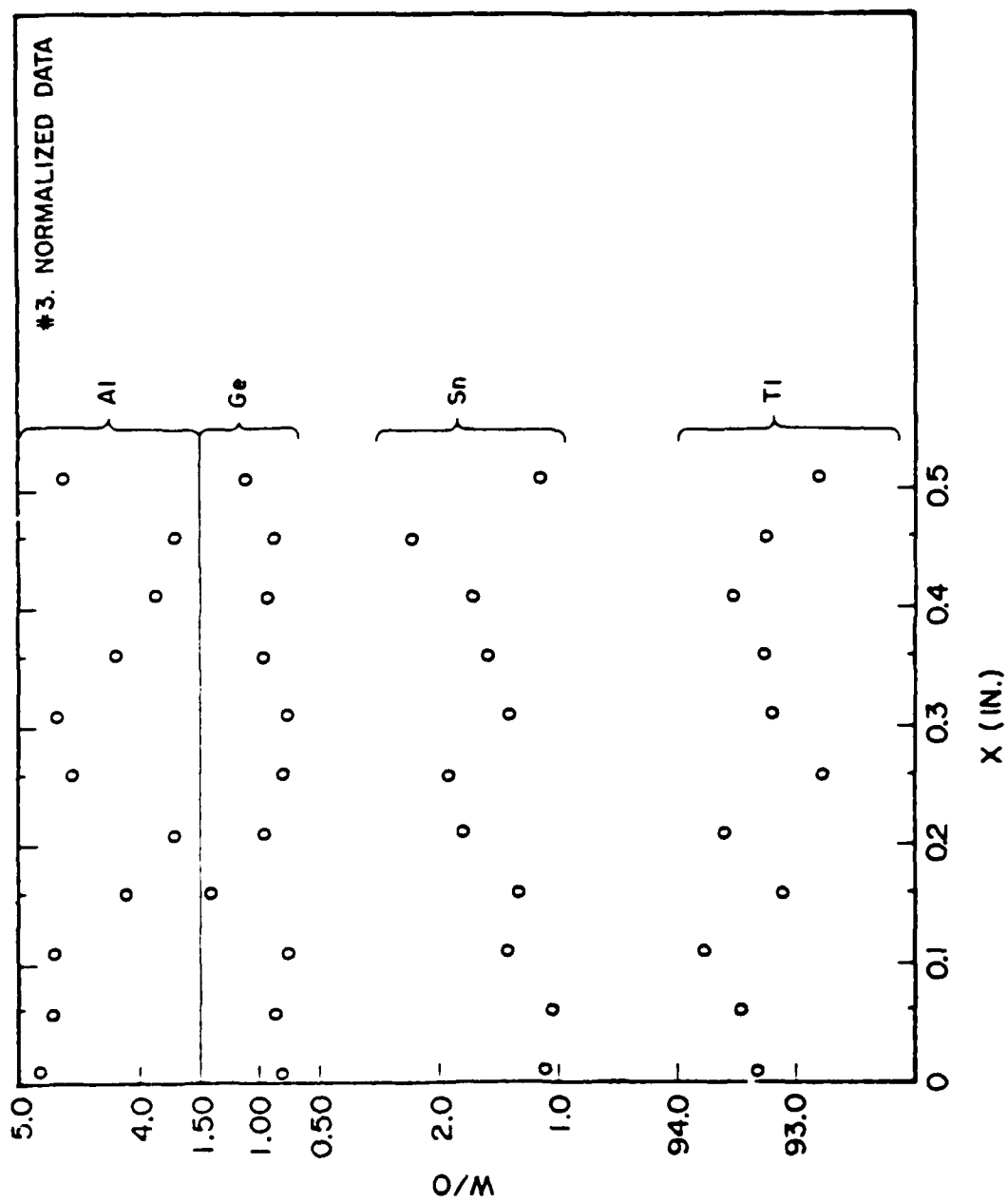


Figure 32. Concentration of Aluminum in Alloy No. 3 Normalized to total calculated concentration of Aluminum in Al, Sn, and Tl in alloy.

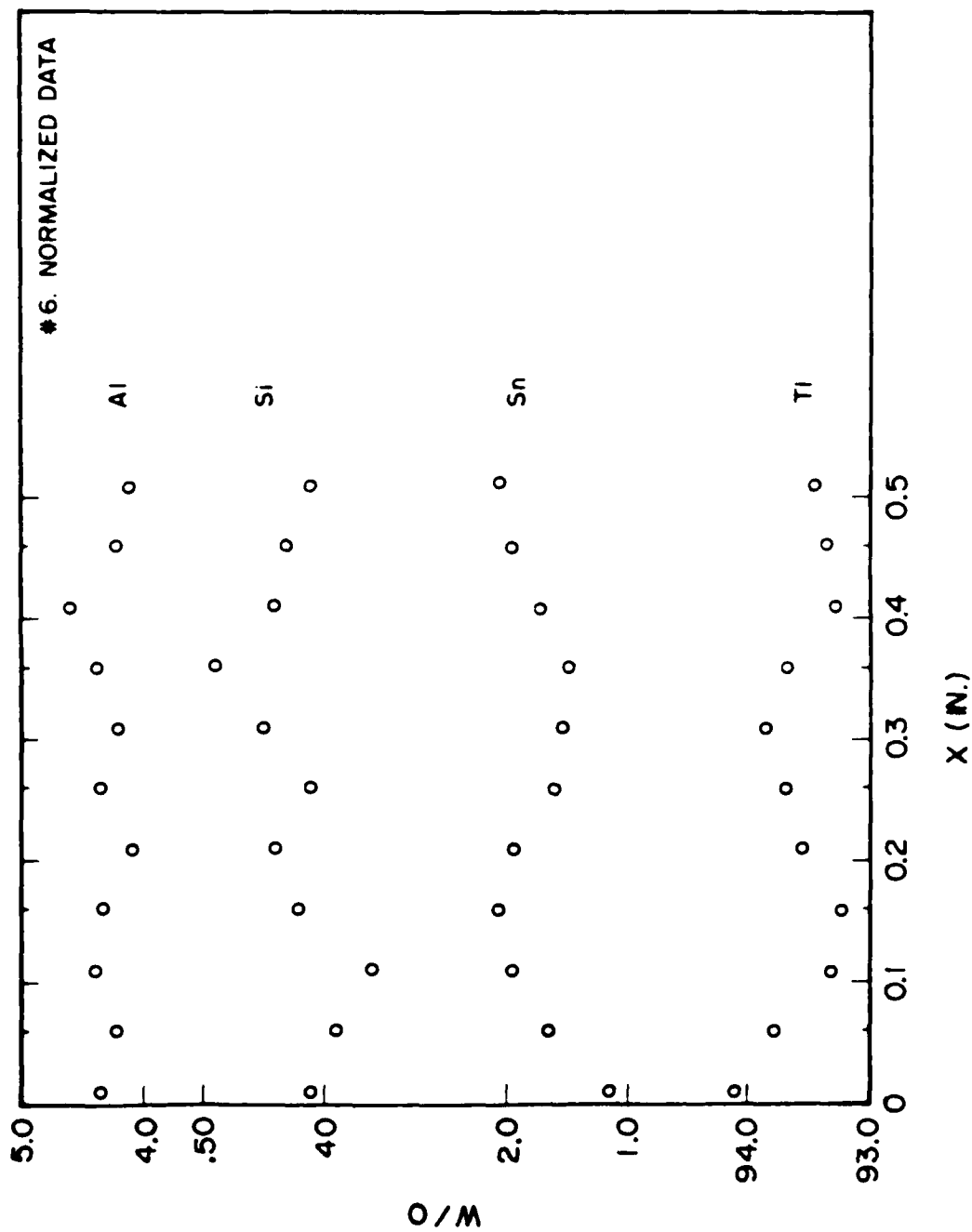


Figure 38. Comparison of normalized data for Al, Si, Sn, and Ti. The data are normalized to the same scale as in Figure 37.

of the specimen, the specimen is tilted somewhat with respect to the radiation axis; variations in beam angle of incidence could produce the artifacts. Spectrometer artifacts also could produce unusual features. These possibilities should be studied. The simplest correction is to physically rotate the specimen 180 degrees and repeat the measurement; in particular, reverses. Sensitivity to beam divergence should be studied by varying the angle used in the FRAMM scan to find concentrations. Also other specimens should be examined to determine whether the in results appear in these specimens as well. Use of different spectrometers, or two spectrometers simultaneously, to collect data could be attempted in order to remove artifacts associated with the spectrometer or spectrometer crystal. The general conclusion at this point is that long-range variations in concentrations may be present. Further study is needed.

Heat-treatment experiments were initiated on the HIP'd material as part of the effort to determine the conditions under which precipitation of Si and Cu will occur. The method employed was to encapsulate the specimen, heat to temperature, hold for 15 min, and then water quench.

The first alloy to be studied was the base material. Figure 39 shows the progression of microstructures obtained between 1825 and 2000°F. The microstructures at 1825 and 1850°F are essentially the same type as those observed in the alloy after HIP'ing and after aging at 1000°F. A major change occurs at 1875°F, where transformed beta is present. The development of the transformed beta continues at 1900°F and 1975°F, where the development is essentially complete. At 1950°F a multi-phase microstructure is observed which may be the result of oxidation of the specimen. The microstructure observed at 1975°F is Widmanstätten-like in appearance. At 2000°F the microstructure displays martensitic structures and is primarily single phase.

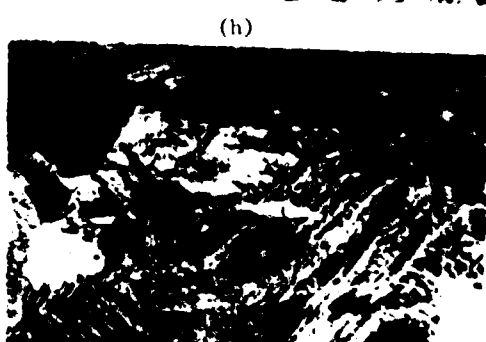
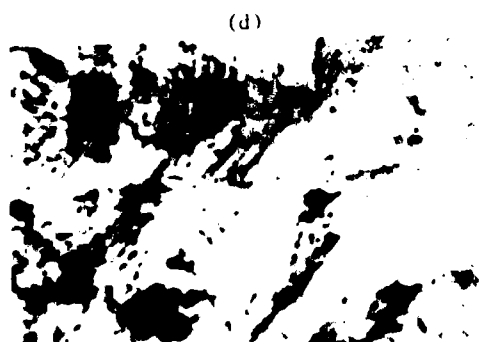
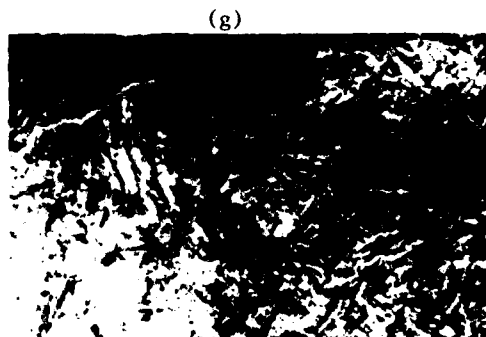
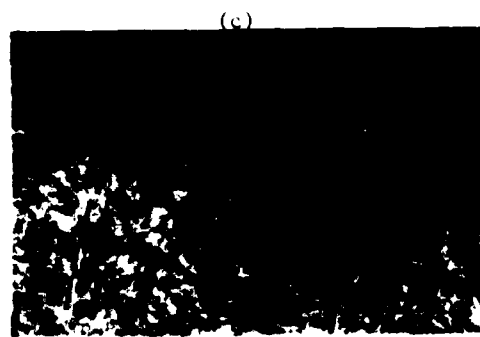
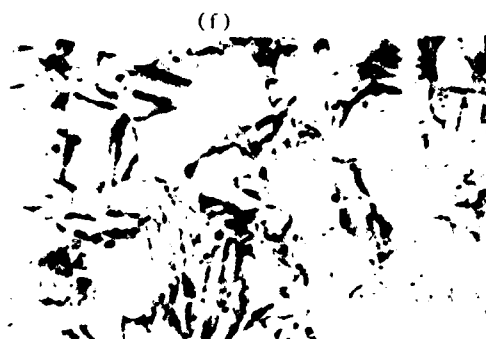
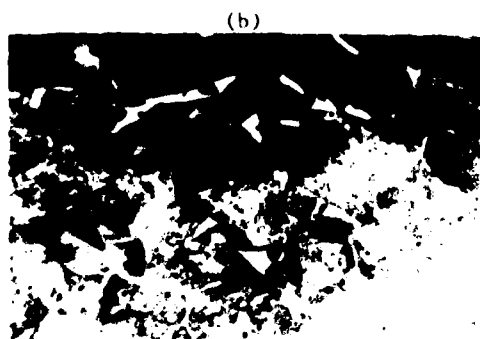
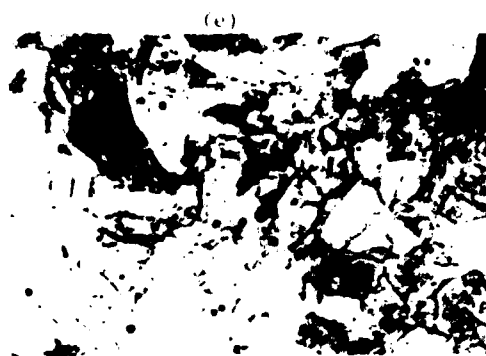
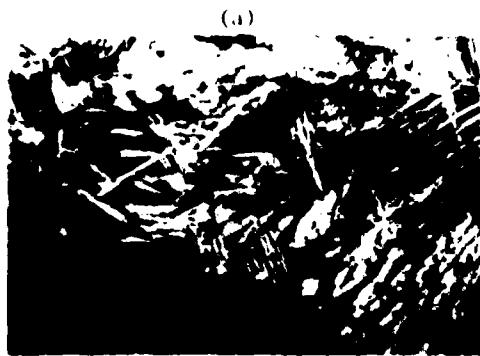


Figure 39. Beta-Transus-determination Results for HIP'd Base Alloy.
(a-h) 1875°F to 2000°F in 25-Deg. Increments. Alpha-
beta transus at 1850°F.

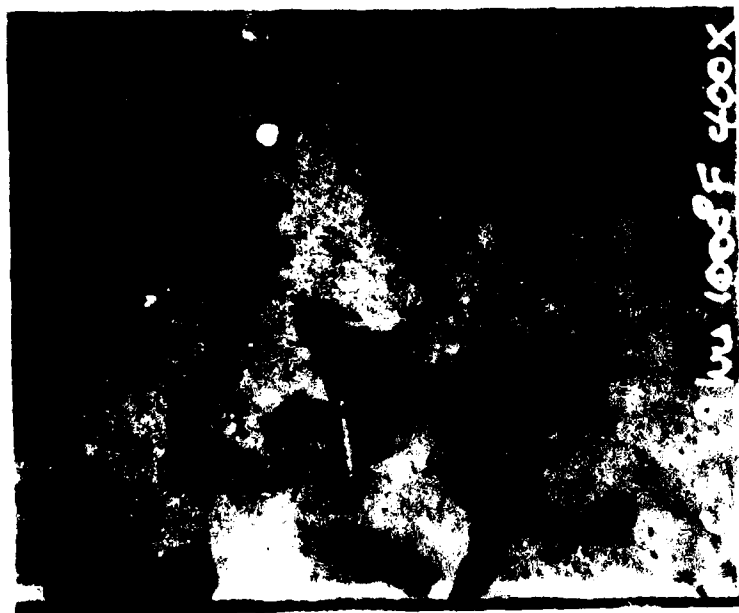
From these data, one concludes that the beta transus occurs at 1850°F. These values for transus temperatures are those expected for Ti-5 Al-2.5Sn according to the literature values (beta at 1875°F).

Aging experiments were conducted to obtain data on changes in microstructure induced by heating. Figures 40-45 show microstructures after heating at 540°C for 29 hr in vacuum, air cooled. These figures are comparisons of CCS and CCSH alloys after aging at 29 hr at 1000°F, air cooled. Generally the new grain structure observed in the HIP'd specimens developed more fully, and the lath boundaries faded. A second-phase was evident on several samples.

Heat Treatment. The three furnaces in Bldg. 32, Room 17, required updating and improvement in the flexibility in control of the temperature profiles attainable. To accomplish this process-controller additions were designed. The Micricon Process Controllers were integrated into the existing control systems on each furnace. The controllers are programmable to allow control of one or two process variables on each furnace.

The Centorr hot press is designed to apply hydraulic uniaxial loads of up to 100,000 lb on a specimen in vacuum at temperatures up to about 1900°F. Figure 46 is a block diagram of the system showing control loops, inputs, and outputs to be attached to and controlled by the controller.

Figures 47 and 48 are block diagrams of the middle Brew and quench Brew furnaces. These were generated in order to identify precisely the control variables required by the programmer controllers. The actual values of the variables (ranges) are listed for each furnace on pages 79 and 80.



(a)



(b)

Figure 40. Microstructures of Ti-5Al-2.5Sn PM Alloy (a) As-Received, Aged 29 hr at 1000°F, (b) HIP'd Material, Same Age Conditions.

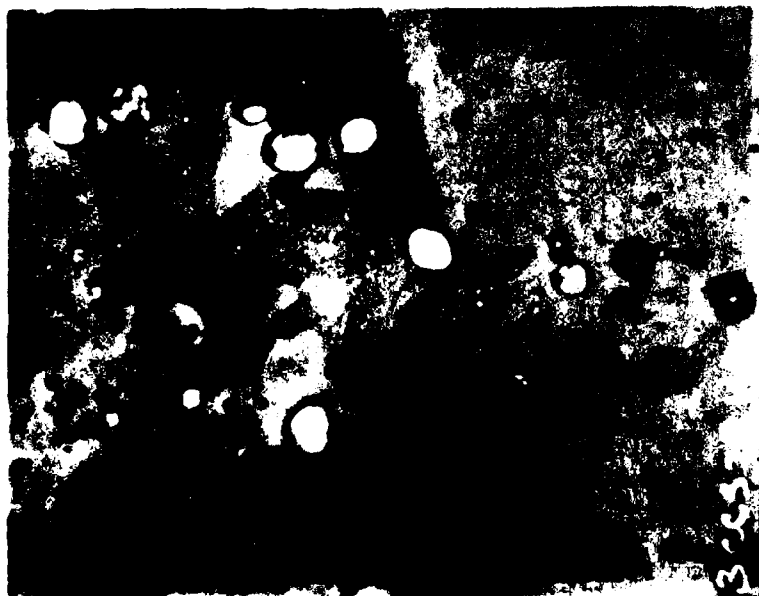


(a)

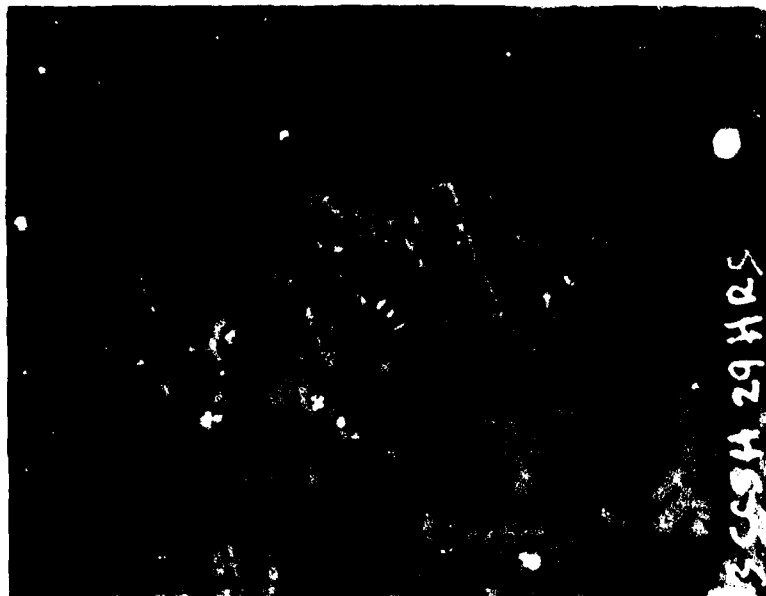


(b)

Figure 41. Microstructures of Ti-5Al-2.5Sn-0.1Si (a) As Received, Age 29 hr at 1000°F, (b) HIP'd, Same Age Conditions.



(a)



(b)

Figure 42. Microstructures of Ti-5Al-2.5Sn-0.5Si (a) As Received, Aged 29 hr at 1000°F, (b) HIP'd, Aged 29 hr at 1000°F.

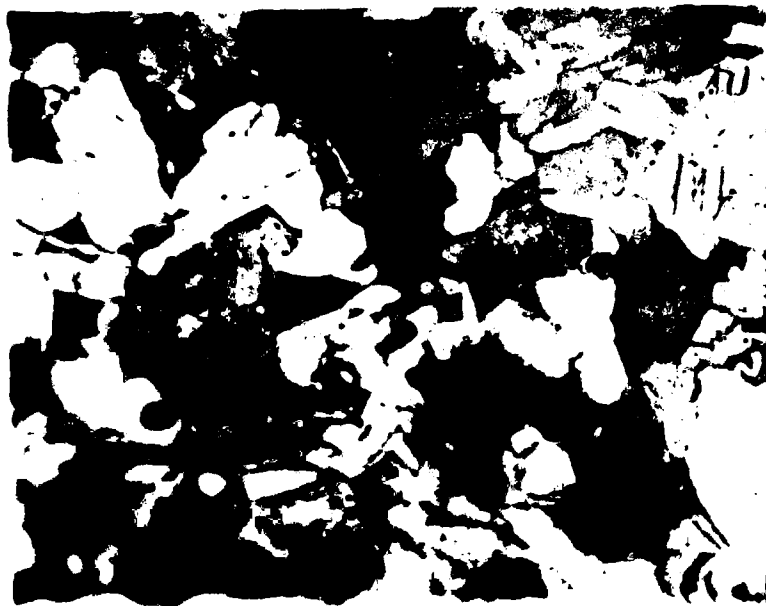


(a)



(b)

Figure 43. Microstructures of Ti-5Al-2.5Sn-0.1Ce (a) As Received, Aged 29 hr at 1000°F, (b) HIP'd, Same Age Conditions.

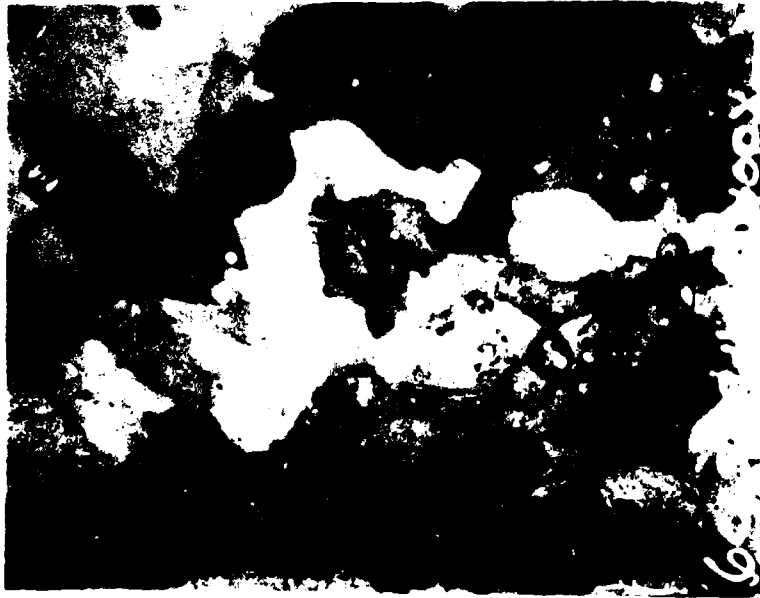


(a)



(b)

Figure 44. Microstructures of Ti-5Al-2.5Sn-0.5Ge (a) As Received, Aged 29 hr at 1000°F, (b) HIP'd, Aged 29 hr at 1000°F.



(a)



(b)

Figure 45. Microstructures of Ti-6Al-2.5Sn-1.7Fe. (a) As Received, Aged 29 hr at 1000°F, (b) HIP'd, Same Age Conditions.

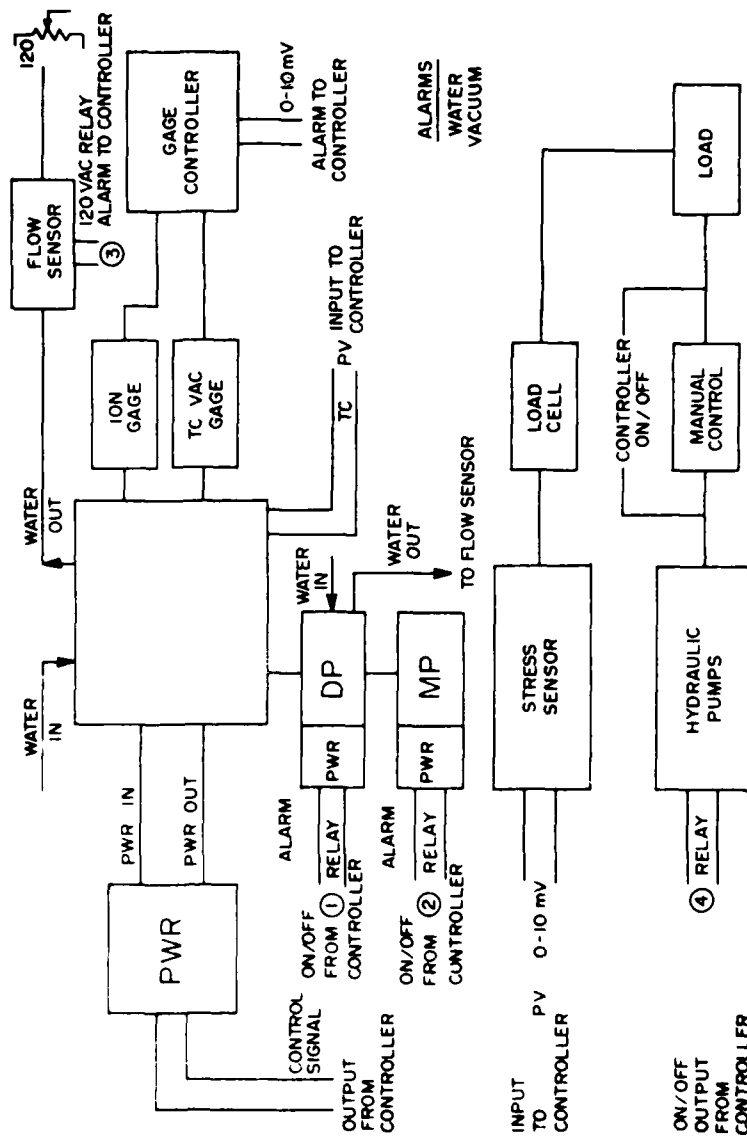
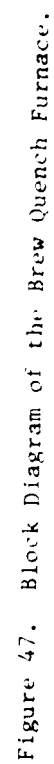


Figure 46. Block Diagram of the Centorr Hot Press.



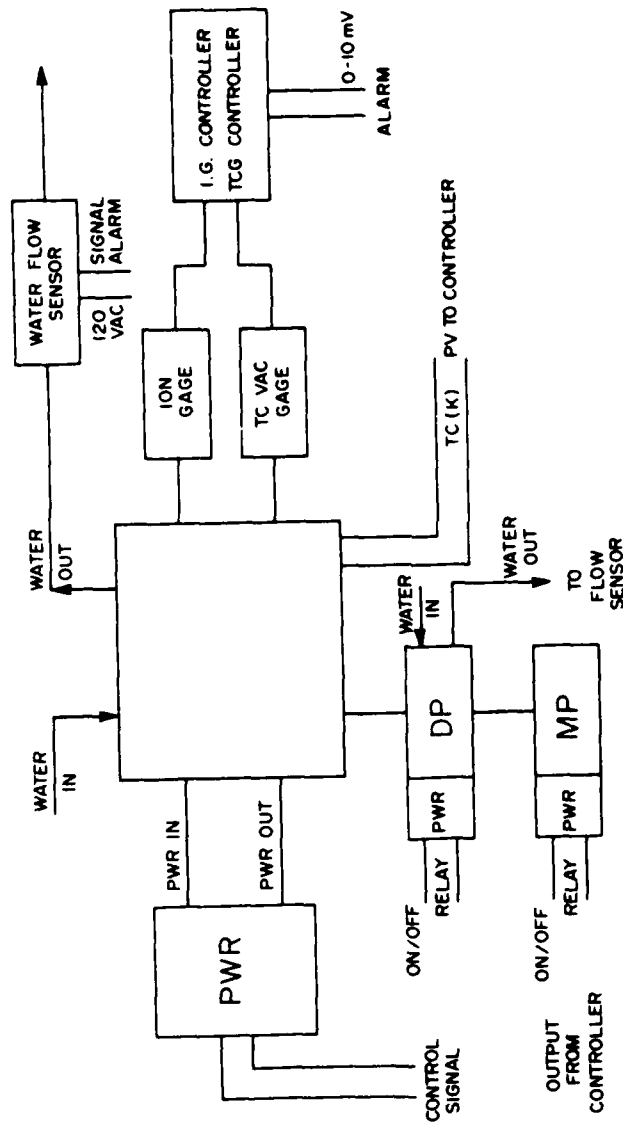


Figure 48. Block Diagram of the Brew Vacuum Furnace.

Once the systems were detailed, a Micricon Programmer Controller was obtained and set up to control the hot press. A representative temperature profile was drawn up, and a program to obtain this profile was written and entered into the programmer. The controller functioned accurately in following the desired profile in terms of turning on/off relays and proportional power output, thereby demonstrating the feasibility of obtaining control of the hot-press system and the others as well.

An example of a control profile is shown in Fig. 49. The temperature regimes are divided into a set of time segments during which events are keyed to occur or the temperature ramps are activated. The programmer controller is programmed to control power to the furnace in a time-proportional control mode for maintaining a setpoint to predetermined high and low deviations. The events (on/off) are actuated by switching designated solid-state relays during the segment. Details of the programming required will not be presented here since these are available in the Micricon manuals.

Integration of the controllers into the furnace systems has been accomplished in such a way that the full manual control has been retained. Either programmed profiles can be run or manual heat treatment can be accomplished. This flexibility is required because of the research/development nature of the work to be accomplished using the furnaces.

LIST OF VARIABLES USED FOR EACH FURNACE

Hot Press:

Sensors

TC-type K
Pressure (vac) 0-10 mV
Stress 0-10 mV LOAD
Water interlock 120V relay

Switches

Mech pump
Diff pump
Heaters

Control-Heaters

Thyratron 0-5.4mA
into 0-3K load

Brew Vacuum:

Sensors

TC- Type K
Pressure (vac) 0-10 mV
Water interlock 120 VAC Relay

Switches

Mech Pump
Diff Pump
Heaters

} 120 VAC RELAYS

Control-Heaters

Phaser power controller Model 646

Brew quench:

Sensors

TC Type K
Pressure (VAC) 0-10 mV
Water interlocks 120 VAC Relay
Furn, DP1, DP2
Quench ready, Quench power

Switches

Mech Pump 1
Diff pump 1
Furnace start
Quench start

Controllers

Varistat-motor driven
(relays)

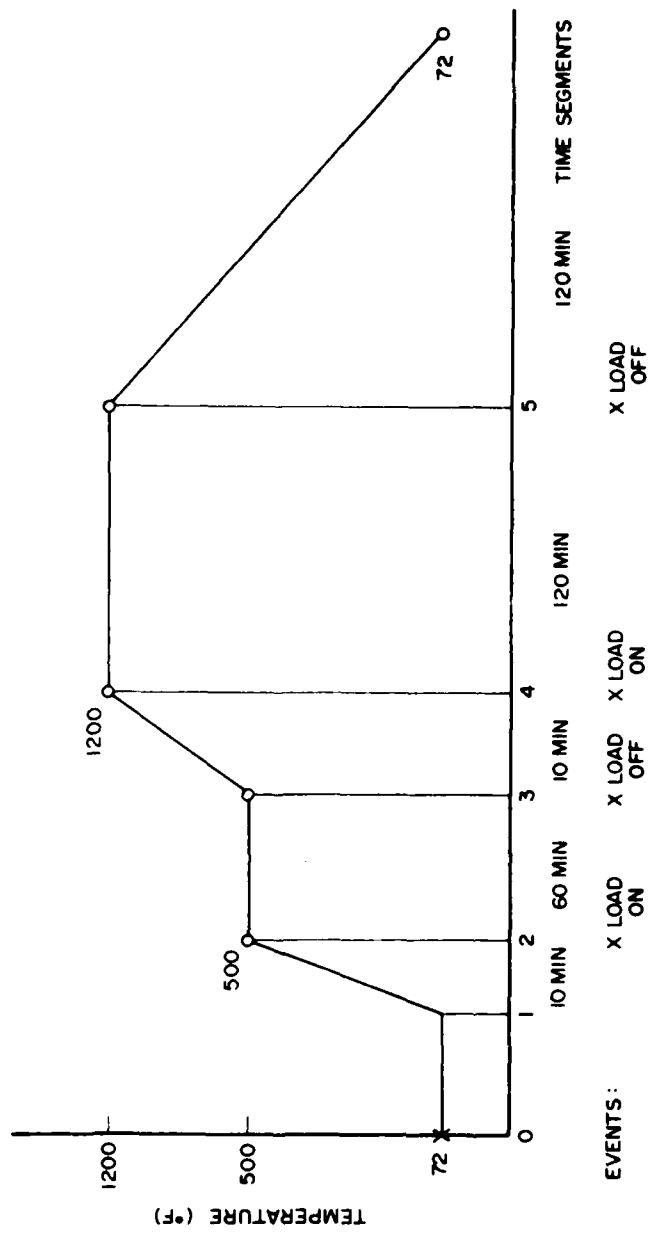


Figure 49. Temperature Profile with Load Events (Hot Press).

REFERENCES

1. E. E. Underwood, Quantitative Stereology (Addison-Wesley Reading, MA, 1970).
2. R. R. Bover, in Powder Metallurgy of Titanium Alloys (F. H. Froes and J. E. Smugeresky, Eds.) (Metallurgical Society of AIME, Warrendale, PA, 1980).

DATE
FILMED
— 8